Challenge Journal of CONCRETE RESEARCH LETTERS

Vol.12 No.4 (2021)

acoustic emission absorption artificial compressive strength neural network concrete corrosion cracking ductility energy absorption ferrocement durability flaky aggregate fly ash fracture mechanical properties mortar reinforced concrete self-compacting concrete silica fume strengthening superplasticizer tensile strength waste disposal water absorption



EDITOR IN CHIEF

Prof. Dr. Mohamed Abdelkader ISMAIL

Miami College of Henan University, China

EDITORIAL BOARD

Prof. Dr. Abdullah SAAND

Prof. Dr. Alexander-Dimitrios George TSONOS

Prof. Dr. Ashraf Ragab MOHAMED

Prof. Dr. Ayman NASSIF

Prof. Dr. Gamal Elsayed ABDELAZIZ

Prof. Dr. Han Seung LEE

Prof. Dr. Zubair AHMED

Prof. Dr. Jiwei CAI

Assoc. Prof. Dr. Meral OLTULU

Dr. Aamer Rafique BHUTTA

Dr. Khairunisa MUTHUSAMY

Dr. Mahmoud SAYED AHMED

Dr. Jitendra Kumar SINGH

Dr. Saleh Omar BAMAGA

Dr. Türkay KOTAN

Quaid-e-Awam University of Engineering, Pakistan

Aristotle University of Thessaloniki, Greece

Alexandria University, Egypt

University of Portsmouth, United Kingdom

Benha University, Egypt

Hanyang University, Republic of Korea

Mehran University, Pakistan

Henan University, China

Atatürk University, Turkey

Universiti Teknologi Malaysia, Malaysia

Universiti Malaysia Pahang, Malaysia

Ryerson University, Canada

Hanyang University, Republic of Korea

University of Bisha, Saudi Arabia

Erzurum Technical University, Turkey

E-mail: cjcrl@challengejournal.com

Web page: cjcrl.challengejournal.com

TULPAR Academic Publishing www.tulparpublishing.com





CONTENTS

Research Articles	
Ballistic strength of aerated concrete Gökhan Durmuş, Sefa Ekinci	114-124
Effects of dry particle coating with nano- and microparticles on early compressive strength of portland cement pastes	125-130
Hediye Yorulmaz, Sümeyye Özuzun, Burak Uzal, Serhan İlkentapar, Uğur Durak, Okan Karahan, Cengiz Duran Atiş	
Strength properties of biopolymer treated clay/marble powder mixtures Zeynep Nese Kurt Albayrak, Banu Altun	131-137
Predictability of concrete damage level by non-destructive test methods Boğaçhan Akça, Süleyman Bahadır Keskin, Aysu Göçügenci	138-150





Research Article

Ballistic strength of aerated concrete

Gökhan Durmuş a,* 🕞, Sefa Ekinci a 🕞

^a Department of Civil Engineering, Gazi University, 06570 Ankara, Turkey

ABSTRACT

In regional studies conducted by the Law Enforcement Agency and the Armed Forces within the scope of counter-terrorism activities, to ensure peace and security throughout the country and for the police and military personnel to provide security services, the need to produce different solutions has arisen in the face of attacks on the security points established at many important points, especially at the entrance and exit points of the cities. In this context, by changing the direction and angle of the wall types made of aerated concrete used in construction techniques, 7 variations were tested on these wall types with materials formed with adhesive mortar+plaster, monolithic elastomer polyurea, and non-Newtonian fluid, and the strength of these materials were tested with BR6 and BR7 bullets. The main purpose of this study was to determine the most suitable material in terms of security parameters in the shortest time and at a low cost and to create a reliable structure for security cabins. At the end of the study, the best results were obtained with the shots made on the narrow surface of the aerated concrete and the shots made on the platform formed with non-Newtonian fluid.

ARTICLE INFO

Article history:
Received 12 July 2021
Revised 9 August 2021
Accepted 18 September 2021

Keywords: Aerated concrete Ballistic Non-Newtonian fluid Monolithic elastomer polyurea

1. Introduction

Throughout the history of the world, humanity has made various studies on how to protect itself against the weapons it has invented, while developing more advanced weapon technologies (Bocetta, 2017). Various materials have been developed and used since animal skins were first used for protection. Steel plates come first among them. Soft ballistic armors made of plates were first tested in Korea in 1860 (Henderson, 2008). During World War II, the development of personal protective armors gained momentum. Later, researchers in Arizona and Illinois have developed a fabric made of silk that could stop bullets fired from certain weapons (Bozdoğan et al., 2015).

Ballistics is a field of mechanics concerned with the launching, flight behavior, and impact effects of projectiles, especially ranged weapon munitions such as bullets, unguided bombs, rockets, or the like. It focuses on explaining the complex event between the time the bullet leaves the muzzle and reaches the target in detail. It is also considered as a special division of applied mechanics

(Plummer, 1940). The standards regarding the protection levels of ballistic protective materials are as follows: NIJ (The US National Institute of Justice) (NIJ Standard-0101.06, 2008) and HOSDB (UK Home Office Scientific Development Branch), these standards have proven their national or international validity and are widely accepted. Apart from this, various military standards have been developed by NATO and the Turkish Standards Institute (TSE EN 771, 2015) However, the fact that regional-based armed conflicts contain different threat elements together with the rapidly developing weapon technology makes it almost impossible to establish and use a single international ballistic protective material standard for all regions. For this purpose, ballistic studies are conducted on different materials.

In these studies, the ballistic performance of the material; is related to the response characteristic in the high-velocity impact region and is proportional to the energy it can absorb during the impact (Mousavi et al., 2020). The material thickness also clearly affects the energy absorbed during impact in some cases (Hsieh et al., 1990) Ballistic protective materials are divided into two

classes as hard and soft protective materials (TDIPC, 2021). Hard protective materials are made of glass, ceramic, and metal. These are used in the form of plates, protective helmets, armors/vests, shields. Soft protective materials, on the other hand, are polymer-based materials consisting of fabric and fabric-like structures (Göksel, 2018; Ayten et al., 2020., Feng et al., 2020). In terms of construction, structural forms consisting of armor/vest steel are used in these materials. In particular, such structures are used at the security points provided for the personnel working in the military and security units to provide safety services in public and private buildings. Although these structures consist of important materials in terms of ballistics and have proven themselves, when it comes to the efficiency, they are not yet at the desired level when compared to other materials in terms of time and cost parameters.

With the developments in construction technology. the behavior of steel, concrete, and other building materials under different loads such as impact has gained even more importance (Jin et al., 2017; Naito et al., 2014). In experimental studies on building materials, test elements produced from high-strength concrete were tested and examined with a free-falling (drop) weight impact test (Feng et al., 2020; Oucif et al., 2021). At the end of the foresaid study, different results were obtained. It was found out that the number of drops depends on the concrete's compressive strength, the damage and deformation types under different impact loads differ from each other, the decrease rate in the maximum acceleration value measured from the test elements with normal and high concrete compressive strength is higher than the decrease rate in the minimum acceleration value, etc. (Kantar et al., 2021; Kaymaz et al., 2018) Different methods have been used depending on the material shape and type in the experiments conducted to see the impact effect (Alkayis et al., 2021) One of them is the studies with explosive materials (Özmen et al., 2018; Verhagen, 1978).

In this study, to provide a safer environment for the police and military personnel providing security services, a study has been conducted on the materials that can be used in structures that can be built to provide protection during terrorist attacks on security points established at many important points such as private and public buildings, especially at the entrance and exit points of the cities. Different wall types were formed by placing the unit volume weight of 600 kg/m³ aerated concrete in different directions. According to the European Standard TS EN 1063 (2002), the BR6, BR7 bullets were fired on the walls produced and the ballistic properties of the walls were examined. Evaluations were made on these walls, which are intended to be used at security points where police and military personnel are employed.

2. Materials and Method

In this study, 7.62x51 mm diameter, and armor-piercing type bullets were fired on two different aerated concretes covered with adhesive mortar (used for bonding aerated concrete), monolithic elastomer polyurea coating material, and non-Newtonian liquid to see different effects.

2.1. Materials

2.1.1. Aerated concrete

In this study, aerated concrete conforming to TS EN 771-4 (2015) standards was used. Technical specifications of aerated concrete are given in Table 1. 6 pieces of 200x600x250 mm³ and 10 pieces of 250x600x250 mm³ aerated concrete were combined with adhesive mortar in 2 blocks and formed as shown in Fig. 1.





Fig. 1. Wall applications made of aerated concrete.

Table 1. Technical sp	ecifications (of aerated	concrete.
------------------------------	----------------	------------	-----------

Behaviour against fire	Dry unit volume weight average	Compressive strength	Shear tie strength	Water vapor permeability coefficient μ	Drying shrinkage	Thermal conductivity value
A1	600 kg/m ³	5 N/mm ²	≥0,3 N/mm ²	5/10	≥0,2 mm/m	≥0,16 W/mK

2.1.2. Adhesive mortar, plaster and mixing water

Normal hardening cementitious adhesive with higher slip-resistance in accordance with TS EN 12004-1 (2017) standards was used both for building aerated concrete walls and for the plaster on their surfaces. The technical specifications of the mortar used are given in Table 2. Additionally, in accordance with the application instructions of the mortar, it was prepared to have 5.6 liters of mains water per 25-kg material. Paid strict attention to ensure that the applied surface mortar was 0.5 cm thick. For the plaster, 4.47 lt of mains water was added to 9-kg material to ensure a thickness of 2-3 mm.

2.1.3. Monolithic elastomer polyurea

Monolithic elastomer polyurea is a material applied using a high-pressure spray system in the range of 54-98°C. It is basically a combination of 4,4'-Diphenylmethane diisocyanate ($C_{15}H_{10}N_2O_2$) and mostly alpha-(2-aminomethyl)-omega-(2-aminomethylethoxy)-poly[oxy (methyl-1,-2-ethanediyl)]. These are polymer components that act as plasticizers, consisting of a reactive component ($C_8H_{20}N_2O_2$). An elastic coating has been used to cover the applied surface and to protect it against bursting, wear and abrasion, and turns into a thick and hard material after application (Izoline, 2021)(Fig. 2).

Table 2. Technical specifications of adhesive mortar.

Behaviour against fire	A1
Dry powder density	$1.4 \pm 0.1 \mathrm{gr/cm^3}$
Initial tensile adhesion strength	≥0,5 N/mm ²
Tensile adhesion strength after immersion in water	≥0,5 N/mm ²
Tensile adhesion strength after heat aging	≥0,5 N/mm ²
Tensile adhesion strength after freezing – thawing cycles	≥0,5 N/mm ²





Fig. 2. Monolithic elastomer polyurea applied on the aerated concrete surface.

2.1.4. Non-Newtonian fluid

It is a powdered material obtained by separating corn using physical methods as a result of processing corn with the wet-milling method (Wikipedia, 2021). It was prepared with 2 kg corn starch and 4 lt water at a mixing ratio of 0.5. It was used by placing it in a 5 cm platform between two glasses placed on the aerated concrete

surface. Additionally, a shooting test was also carried out on a 16 cm wide platform consisting of a mixture of 2.5 kg of corn starch and 5 lt of water, which was placed on the aerated concrete surface of a different size. It was also aimed to benefit from its properties of behaving like a liquid and solid material when velocity-dependent force is applied to the non-Newtonian fluid mixture (Fig. 3).





Fig. 3. Starch in the platform applied on the aerated concrete surface.

2.1.5. G3 rifle and ballistic bullet

Shooting studies were carried out on the materials conducted by expert personnel using a G3 assault rifle,

which is loaded with 7.62 mm magazine and functions automatically and semi-automatically with the roller-delayed blowback. The characteristics of the firearm are given in Table 3.

Table 3. Technical specifications of the G3 assault rifle.

Cartridge	7.62x51 mm
Length	102 cm
Target range scaling	100-200-300-400 m
Maximum Firing Range	3700 m
Effective Firing Range	400 m
Mass (without magazine)	4.25 kg
Magazine Capacity	20
Muzzle velocity	800 m/s
Rate of fire	500-600 rounds/min

To test the BR6 and BR7 ballistic levels, during the shooting, different numbers of armor-piercing bullets of 7.62x51 mm diameter and type (M61) designed for

lightly armored targets such as steel vests, bulletproof glass and light armored vehicles were used, as shown in Fig. 4.





Fig. 4. G3 assault rifle and armor-piercing bullet.

2.2. Method

Aerated concrete, which have a compressive strength of 5 N/mm² and are used in the construction of exterior and interior infilled walls in construction systems, and also are used as a load-bearing outer and inner wall material in masonry structures, were formed as double row blocks by adhering with cement-based mortar material with a dry powder density of 1.4 gr/cm³ and increased vertical slip resistance. The surfaces and direction of the formed aerated concrete blocks were changed and covered separately by using materials such as mortar-plaster, starch, and monolithic elastomer polyurea that protects against impact and pressure. The aerated concrete

blocks formed with these materials were shot using a G3 assault rifle with a 7,62x51 mm diameter and type (M61) armor-piercing bullet according to the ballistic standards. The ballistic level table of the bullets is given in Table 4.

The shooting test was carried out following the instructions specified in TS EN 1063 (2002) by shooting with a G3 assault rifle (bullet angle of 90 degrees and a shooting distance of 10 m) on aerated concrete of different sizes, coating materials and directions, which was fixed with supporting products. A picture of the shooting range is shown in Fig. 5. The gradual summary of the article work program is shown in Table 5 in accordance with the modellings.

Table 4. Ballistic levels table.

CEN (Committee European Normalization) BS/EN 1063 Strength Standards											
Level Weapon type Calibre Bullet type Mass (gr) Shooting distance Projectile velocity (m) Shots Distance bet shots (mm)											
BR6	Rifle	7.62 x 51mm	FJ1 / PB / SC	9.5 ± 0.1	10.00 ± 0.5	830 ± 10	3	120 ± 10			
BR7	Rifle	7.62 x 51mm	FJ2 / PB / HCI	9.8 ± 0.1	10.00 ± 0.5	820 ± 10	3	120 ± 10			



Fig. 5. Shooting range setup.

Table 5. Shooting experiment modeling.

Experiment		Shooting direction to the wall		Aerated concrete dimensions (mm)		Mater		Bullet type		Number of shots		
Experiment		Horizontal	Vertical	20x60x25	25x60x25	Mortar +Plaster	Monolithic elastomer polyurea	Starch	BR6	BR7	BR6	BR7
Chapting 1	1-a	\checkmark			✓	✓			✓	\checkmark	3	1
Shooting-1	1-b	\checkmark			✓		✓		✓	\checkmark	3	3
Chartina 2	2-a		✓		✓	✓			✓	✓	1	1
Shooting-2	2-b		✓		✓		✓		✓	✓	1	1
Shooting-3		√		✓		✓			✓	✓	3	1
Character 4	4-a	✓			✓	✓		√	-	✓	-	1
Shooting-4	4-b	✓		✓		✓		✓	-	✓	-	1

The study is structured in 4 sections as indicated in Table 5. Shooting-1: It shows 2 different shooting tests carried out to see the effect of the material applied to the surface of the aerated concretes with the same thickness in the horizontal direction. Shooting-2: It shows 2 different shooting tests carried out to see the effect of the material applied to the surface of the aerated concretes with the same thickness in the vertical direction. Shooting-3: It shows the shooting test carried out to see the effect of the material applied to the surface of the aerated concrete (depending on the thickness) which was formed in a double row. Shooting-4: It shows 2 different shooting tests carried out to see the effect of the material of different thicknesses applied on the surface of 20 cm and 25 cm thick aerated concretes in the horizontal direction.

2.2.1. Shooting tests during the study

In the Shooting-1 part of the study, a total of 10 rounds of BR6 and BR7 bullets were shot on two different walls,

on the horizontal wide surface of the aerated concrete. The schematic representation of the sample coated with adhesive mortar-plaster is shown in Fig. 6a, and the sample coated with monolithic elastomer polyurea is shown in Fig. 6b.

When Fig. 6 is examined: a) 3 rounds of BR6 bullets were shot on the upper zone and 1 round of BR7 bullet was shot on the lower zone; b) 3 rounds of BR6 bullets were shot on the upper zone and 3 rounds of BR7 bullets were shot on the lower zone.

When Fig. 7 is examined; in both Shooting-2a and Shooting-2b, 1 round of BR6 bullet was shot on the upper zone and 1 round of BR7 bullet was shot on the lower zone.

In the Shooting-3 part of the study, a total of 4 rounds of BR6 and BR7 bullets were shot on a double row 20 cm thick aerated concrete wall, on the horizontal wide surface. Its schematic representation is shown in Fig. 8.

In Fig. 8, 3 rounds of BR6 bullets were shot on the upper part of the aerated concrete and 1 round of BR7 bullet was shot on the lower part of the aerated concrete.

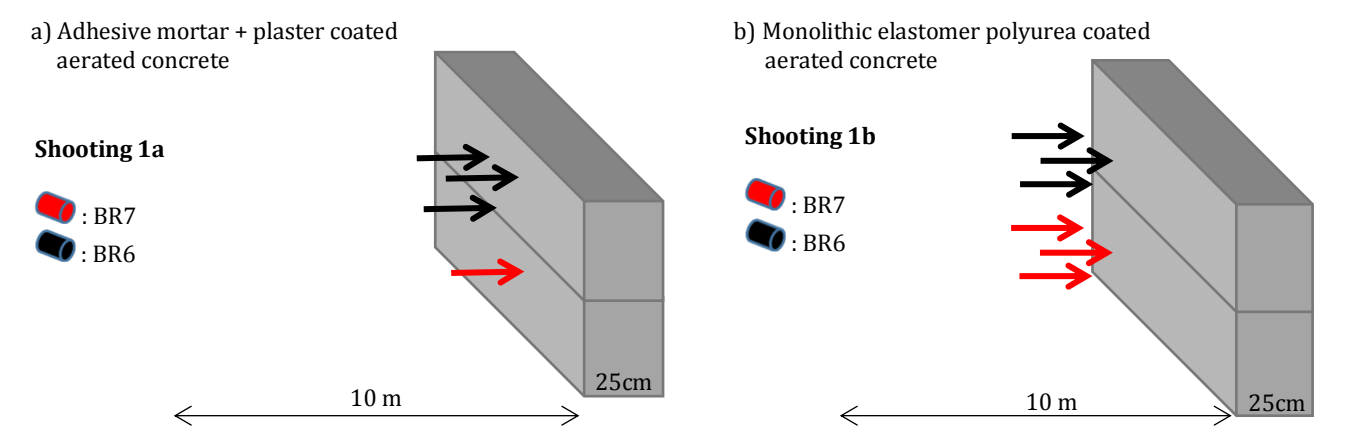


Fig. 6. Schematic representation of the shots fired on the two wide and short surfaces of the aerated concrete wall.

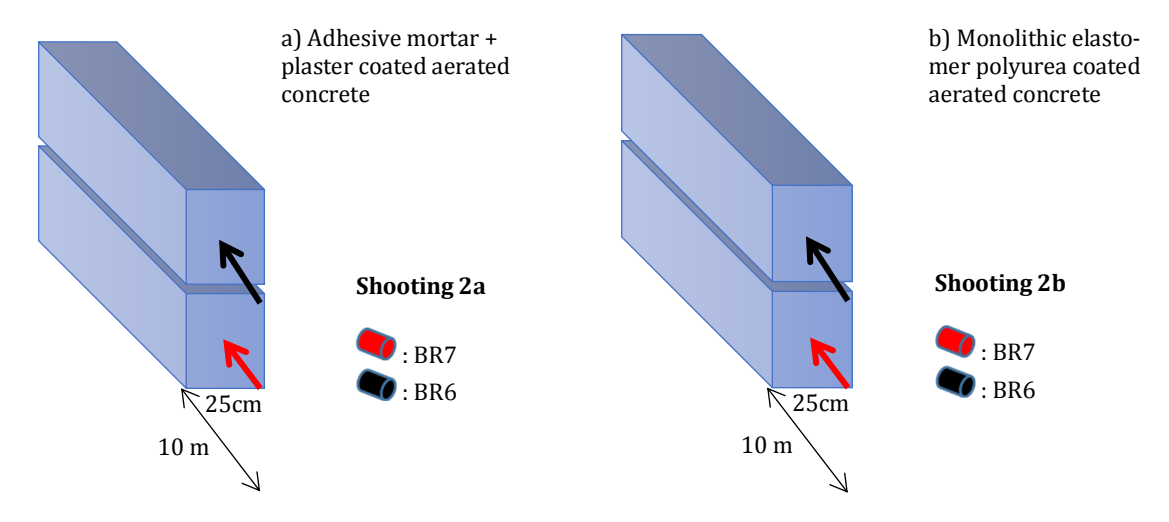


Fig. 7. Schematic representation of the shots fired on the two short surfaces of the aerated concrete wall.

Mortar-plaster coated aerated concrete

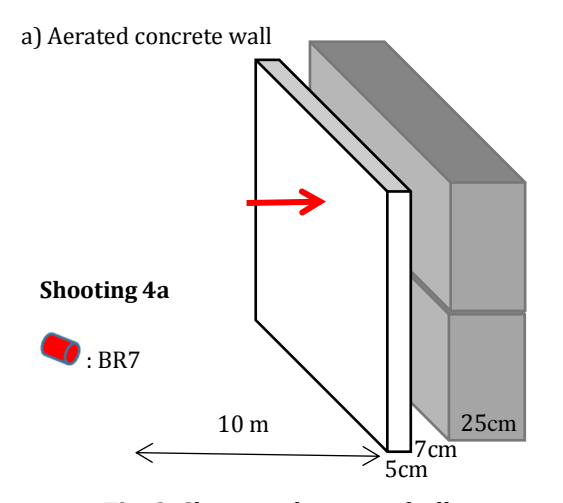
Shooting 3
: BR7
: BR6

10 m
20cm
20cm

Fig. 8. Adhesive mortar + plaster shooting diagram.

In the Shooting-4 part of the study, a total of 2 rounds of BR7 bullets were shot on the starch-filled platforms in front of the horizontal wide surface of the aerated concrete, on the walls made of 20 cm and 25 cm thick aerated concrete. Its schematic representation is shown in Fig. 9.

BR7 bullet was shot on the starch in the platform with a distance of 7 cm to the aerated concrete and a width of 5 cm.



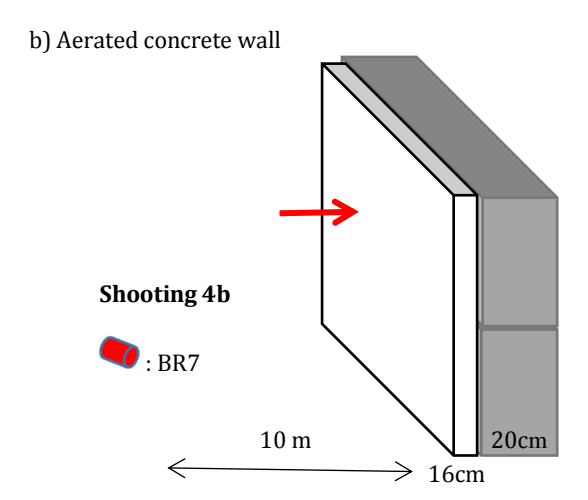


Fig. 9. Shooting diagram of adhesive mortar-plaster and non-Newtonian liquid in front of it.

3. Findings and Discussion

3.1. Shooting test-1

As a result of the shooting tests performed on wide surfaces of aerated concrete coated with different coating materials such as adhesive mortar-plaster and monolithic elastomer polyurea;

- The aerated concrete sample coated with adhesive mortar-plaster was shot with 3 rounds of BR6 bullets and 1 round of BR7 bullet in a controlled manner, according to the bullet exit status. In the examination carried out after the shooting, perforation was observed on the back surface of the aerated concrete as a result of the damage caused by the bullets. To examine the effect of the bullet on the aerated concrete, the aerated concrete was divided into 2 equal parts of 12.5 cm and their measurements were taken. The measurements taken are given in Table 6.
- The aerated concrete sample coated with monolithic elastomer polyurea was shot with 3 rounds of BR6 bullets and 3 rounds of BR7 bullets in a controlled manner, according to the bullet exit status. In the examination carried out after the shooting, perforation was observed on the back surface of the aerated concrete as a result of the damage caused by the bullets. To examine the effect of the bullet on the aerated concrete, the aerated concrete was divided into 2 equal

parts of 12.5 cm and their measurements were taken. The measurements taken are given in Table 6.

In Table 6, the positions of the bullets in both aerated concretes are indicated by measuring the distance they change both in height and horizontally. When this table is examined, it is seen that the BR6 and BR7 bullets do not follow a linear path, and the materials used on the surface affect the movement of the bullets. Especially in aerated concrete coated with monolithic elastomer polyurea material, it was determined that the displacements of the bullets in the shots fired with BR7 bullets were higher than the adhesive mortar-plaster. This can be explained by the resistance of the monolithic elastomer polyurea and the effect of the BR7 bullet. However, the fact that the bullets exited from the back surface in both aerated concrete showed us that such a form could not be built.

3.2. Shooting test-2

As a result of the shooting tests performed on narrow surfaces of aerated concrete coated with different coating materials such as Adhesive Mortar-plaster and Monolithic elastomer polyurea (by changing its direction);

 The aerated concrete sample coated with adhesive mortar-plaster was shot with 1 round of BR6 and 1 round of BR7 bullet in a controlled manner, according to the bullet exit status. In the examination carried out after the shooting, no perforation was observed on the back surface of the aerated concrete as a result of the damage caused by the BR6 bullet. In the shot fired with the BR7 bullet, no perforation was observed and the bullet exited at a distance of 25 cm from the back surface. In order to examine the effect of the bullet on the aerated concrete, the aerated concrete was divided into 4 pieces of 10/15/10/25 cm and their measurements were taken. The measurements taken are given in Table 7.

 The aerated concrete sample coated with monolithic elastomer polyurea was shot with 1 round of BR6 bullet and 1 round of BR7 bullet in a controlled manner, according to the bullet exit status. In the examination carried out after the shooting, it was observed that the bullet advanced up to 41 cm from the surface of the aerated concrete in the shot fired with the BR6 bullet but no perforation occurred on the back surface as a result of the damage done by the bullet. In the shot fired with the BR7 bullet, no perforation was observed and the bullet exited at a distance of 17.5 cm from the back surface. To examine the effect of the bullet on the aerated concrete, the aerated concrete was divided into 4 pieces of 10/15/15/25 cm and their measurements were taken. The measurements taken are given in Table 7.

Table 6. Effect of the bullets on the wide surface of the aerated concrete (measurements were taken from the front surface and left surface).

Surface coating		Adhesive mo	ortar-plaster		Monolithic elastomer polyurea			
Protection level	BI	BR6		BR7		BR6		R7
Measurement (cm)	Front surface	Left surface	Front surface	Left surface	Front surface	Left surface	Front surface	Left surface
	35.0	16.0			37.0	15.0	16.0	25.5
Entrance (surface)	39.0	20.5	23.5	31.5	40.0	25.0	8.5	35.0
(surface)	33.5	33.0			39.5	33.5	19.0	28.5
	33.0	15.0			37.5	14.5	15.0	27.5
Middle (12.5 cm)	38.0	19.5	26.0	32.5	39.5	26.0	10.5	29.5
(12.5 cm)	32.5	32.0			40.0	33.5	20.5	36.0
	31.0	14.0			37.0	13.5	19.0	27.5
Exit (25 cm)	35.0	18.5	26.0	34.5	37.5	26.0	15.5	34.0
(25 cm)	30.5	31.5			39.0	32.5	26.0	40.0

Table 7. The effect of the bullet on the aerated concrete narrow surface (measurements were taken from the front surface and left surface).

Surface coating		Adhesive mo	ortar-plaster		Monolithic elastomer polyurea				
Protection level	BR6 Front Left surface surface		BR7		BI	R6	BR7		
Measurement (cm)			Front Left surface		Front surface	Left surface	Front surface	Left surface	
Entrance (surface)	37.5	7.0	15.5	9.0	37.0	12.5	15.5	14.5	
10 cm	37.0	7.0	14.5	9.0	37.0	12.5	15.0	14.5	
25 cm	38.0	7.0	12.0	5.0	34.0	13.0	13.0	6.5	
35 cm	39.0	8.0	10.0	1.5	33.5	11.5	9.5	3.0	

In Table 7, the positions of the bullets in both aerated concretes are indicated by measuring the distance they change both in height and horizontally. When this table is examined, it has been determined that the height and displacements on the aerated concrete coated with both materials are higher in the shots fired with BR7 bullets. As a result of the long trajectory of the projectile in shots fired on the narrow surface and the hollow structure of the aerated concrete, BR6 bullets could not exit through the aerated concrete coated with adhesive mortar + plaster and monolithic elastomer polyurea, while BR7 bul-

lets exited from the side surface. The fact that the bullets did not exit from the back surface in both aerated concretes showed that such a structure could be formed, however, it is thought that building a form so that the bullet remains in the aerated concrete and conducting a study in this direction will yield better results.

In the study conducted with both coating materials, it was observed that the studies performed with monolithic elastomer polyurea were better than the adhesive mortar + plaster, but did not yield the desired result, according to the data in Tables 6 and 7.

3.3. Shooting test-3

3 rounds of BR6 bullets and 1 round of BR7 bullet were shot on the surface coated with mortar-plaster, which was obtained by combining 2 rows of aerated concrete with adhesive mortar. In the examination

Entrance

(surface)

Exit

(25 cm)

made after the shooting tests, it was seen that as a result of the damage caused by the bullets, perforation did not occur on the back surface of the aerated concrete in all shots. To examine the effect of the bullet on the aerated concrete, the entrance and exit hole of the bullet were measured. The measurements are given in Table 8.

	(iiieasai eiii	01100 11 01 0 0011011			14.00).					
	Surface coating	Adhesive mortar-plaster								
	Protection level	ВІ	R6	BR7						
	Measurement (cm)	Front surface	Left surface	Front surface	Left surface					
Ì		23.5	23							

25.5

19.0

32.0

30.0

26.5

39.5

47.5

12.5

33.5

40.5

Table 8. The effect of the bullet on the aerated concrete formed in double rows (measurements were taken from the front surface and left surface).

In Table 8, the positions of the bullets in both aerated concretes are indicated by measuring the distance they change both in height and horizontally. When this table is examined, it is seen that the BR6 and BR7 bullets do not follow a linear path. The fact that the bullets had exited from the back surface in the aerated concrete showed us that such a form could not be built. Although 2 rows of 20 cm thick aerated concrete were formed and the thickness was 40 cm, it was understood that the thickness had no effect on an aerated concrete wall built in such a structure.

3.4. Shooting test-4

As a result of the shooting tests performed on the starch-coated materials placed in front of the adhesive mortar-plaster coated surface on the wide surfaces of the aerated concrete;

• The starch inside the platform with a distance of 7 cm to 25 cm thick aerated concrete and a width of 5 cm was shot with 1 round of BR7 bullet. In the examination made after the shooting, it was observed that the bullet penetrated 13 cm from the moment it entered the surface, and no perforation occurred on the back surface of the aerated concrete. To examine the effect of the bullet on the aerated concrete, the aerated concrete was divided into 2 equal parts from their joints

and their measurements were taken. The measurements are given in Table 9.

37.5

31.5

16.5

25.0

• The material containing starch with a diameter of 16 cm in front of 20 cm thick aerated concrete was shot with 1 round of BR7 bullet. In the examination made after the shooting, it was observed that the bullet penetrated 14 cm from the moment it entered the surface, and no perforation occurred on the back surface of the aerated concrete. To examine the effect of the bullet on the aerated concrete, the aerated concrete was divided into 2 equal parts of 10 cm and their measurements were taken. The measurements are given in Table 9.

In Table 9, the positions of the bullets in both aerated concretes are indicated by measuring the distance they change both in height and horizontally. When this table was examined, in the shots fired with BR7 bullets, it was seen that the heights and displacements on both aerated concretes were in different directions. In structures created with non-Newtonian fluids, the fact that the bullets did not exit from the back surface in both aerated concretes makes it the best choice to build such a form. Compared with other shooting experiments, the fact that it kept the bullet inside showed that this form was successful and it would be appropriate to carry out studies in this direction so that it could be used in structures to be built (Fig. 10).

Table 9. The effect of the bullet on the aerated concrete formed with starch (measurements were taken from the front surface and left surface).

Surface Coating	Platform	Starch	Surface Coating	Platform Starch		
Protection Level	BR	7	Protection Level	BR7		
Measurement (cm)	Front surface	Left surface	Measurement (cm)	Front surface Left surface		
Entrance (surface)	28.0	38.5	Entrance	22.5	25.5	
13 cm	33.0 40.0		10 cm	21.5	22.5	





Fig. 10. Effect of shots fired on starch coated aerated concrete.

4. Conclusions

In the study, to examine the impact effect of aerated concrete and to measure its ballistic resistance against BR6 and BR7 bullets, the effect of thickness, direction, and different materials applied to the surface was examined by using 4 different stages. The evaluations were made as a result of the cuts made on the aerated concrete, the movements of the bullet on the aerated concrete surface, and the entrance-exit hole damages.

- It is very difficult to generalize the results due to the fact that such studies on aerated concrete are conducted for the first time and the studies in this field are extremely limited. However, this study is thought to be a basis for future studies.
- The hollow structure of aerated concrete has affected the path the bullets followed inside the aerated concrete. When the displacement and height changes in the figures were examined, it was seen that there was no linear movement. This situation was effective in the fact that the bullet could not exit through the back surface after entering the aerated concrete, especially in the shots fired on the narrow surface and the shots fired on the starchy surface.
- As a result of the shooting tests, Shooting-1, 1-a, 1-b and Shooting-3 were unsuccessful because the bullets exited through the back surfaces and could not show the desired strength performance. In the 2-a and 2-b shooting tests carried out in Shooting-2, the BR-6 bullets did not perforate, and the shots made with the BR-7 bullets exited from the side surface before reaching the back surface. Compared to Shooting-1 and Shooting-3, it can be said that it was a successful test, but the study can be expanded to further improve this form and keep the bullets inside. Tests carried out on the structures built in Shooting-4, 4-a and 4-b are the most successful ones. It was able to keep the bullet inside and there was no exit from the back surface. This study was more reliable and successful than the other 3 studies.
- In the application of adhesive mortar-plaster applied to the wide surface of the aerated concrete, it was determined that even if the thickness of the aerated concrete was increased, it could not prevent the bullet from exiting. In the aerated concretes created with the application of monolithic elastomer polyurea, it has been observed that, unlike the large bullet entrances and exits in the adhesive mortar-plaster application, the bullet is in the form of small scratches at the entrance and exit points, and the bullet exits when the monolithic elastomer polyurea coating is removed. The monolithic elastomer polyurea absorbed the energy in the parts where the projectile entered and exited the aerated concrete and kept the material together without scattering. It is thought that it would be appropriate to use a material of this nature against explosions, etc., instead of an armed attack.
- In the shots fired on the narrow surface, there was no exit from the back of the aerated concrete. It was observed that BR7 bullets exited from the side surface on both the adhesive mortar-plaster and monolithic elastomer polyurea coated surfaces. In a structure to be formed, in order to provide protection, it will be advantageous to form the direction of the aerated concrete to be used in the narrow surface direction.
- Studies on starch-coated surfaces have been more successful than other materials applied. In particular, the resistance of the oobleck mixture (non-Newtonian fluid) created with a mixture of water and starch on the aerated concrete surface against the impact, and the fact that the BR7 bullets did not exit after the shots fired on the wide surface, showed that a structure formed suitably with this material would be appropriate. Especially in the setup built with the starch platform, the 7 cm gap between the aerated concrete and the setup was also effective. When the displacement and height changes were examined, it was seen that the bullet was displaced more in the starch formed with the platform. This situation can be explained by the fact that the projectile was displaced during the process after hitting the platform, especially in a hollow environment.

Within the scope of this study and the scope of a structure to be formed with aerated concrete, with the direction of the aerated concrete, the gap structure that can be formed in front of the aerated concrete (with building materials such as stone wool, etc.) and a form of starch suitable for building materials, the establishment of police and military security points will be both time and cost-effective.

Acknowledgements

I would like to thank the General Directorate of Security, Construction Real Estate Department and Criminal Department, Turkish YTONG Industry Inc. and Izoneks İnşaat Yapı Market companies for their valuable information and assistance during my studies in this article, and for their product support and contributions to my experimental studies.

REFERENCES

- Alkayiş MH, Başyiğit C (2021). Effect of fiber additive on concrete impact strength. European Journal of Science and Technology, 24, 455-462.
- Ayten Aİ, Taşdelen MA, Ekici B (2020). An experimental investigation on ballistic efficiency of silica-based crosslinked aerogels in aramid fabric. Ceramics International, 46(17), 26724-26730.
- Bocetta S (2017). The History of Body Armor, From Medieval Times to Today. https://smallwarsjournal.com/jrnl/art/the-history-of-body-armor-from-medieval-times-to-today. Downloaded on 28.04.2021
- Bozdoğan F, Üngün S, Temel E, Mengüç G (2015). Textiles used for balistic protection, their properties and balistic performance tests. Journal of Textiles and Engineer, 11(98), 84-103.
- Feng J, Sun W, Wang L, Chen L, Xue S, Li W (2020). Terminal ballistic and static impactive loading on thick concrete target. Construction and Building Materials, 251, 118899.
- Göksel B (2018). Aramid Fiber Tib2 Reinforcement at Different Fiber Orientation Angles, Mechanical and Ballistics Investigation, Ph.D. thesis, Kırıkkale University, Kırıkkale, Turkey.
- Henderson J (2008). Ballistic Body Armor Protecting. The Protectors. Strategic Standardization, 1-18,
- Hsieh C, Mount A, Jang B, Zee R (1990). Response of polymer composites to high and low velocity impact. Proceedings of the 22nd International SAMPE Technical Conference, 14-27.
- Izoline (2021). http://www.izolinex.com/line-x.html.
- Jin X, Jin T, Su B. Wang Z. Ning J, Shu X (2017). Ballistic resistance and energy absorption of honeycomb structures filled with reactive powder concrete prisms. Journal of Sandwich Structures & Materials, 19(5), 544-571.
- Kantar E, Arslan A, Özgür A (2011). Effect of concrete compressive strength variation on impact behaviour. Journal of the Faculty of Engineering and Architecture of Gazi University, 26(1), 115-123.
- Kaymaz, K, Arıcı E (2018). The effect of mechanical properties of concrete on impact strength. Gümüşhane University Journal of Science and Technology Institute, 8(2) extra, 106-111.
- Mousavi MV, Khoramishad H (2020). Investigation of energy absorption in hybridized fiber-reinforced polymer composites under high-velocity impact loading. International Journal of Impact Engineering, 146, 103692.
- Naito C, States J, Jackson C, Bewick B (2014). Crumb rubber concrete performance under near-field blast and ballistic demands. Journal of Materials in Civil Engineering, 26(9), 04014062.
- NIJ Standard-0101.06 (2008). America Ballistic Resistance of Body Armor, Washington, USA.
- Oucif C, Kalyana Rama JS, Shankar Ram K, Abed F (2021). Damage modeling of ballistic penetration and impact behavior of concrete panel under low and high velocities. Defence Technology, 17(1), 202-211.
- Özmen H, Soyluk K, Özgür A (2018). The effect of concrete strength on the structural behaviour of reinforced concrete buildings under explosive-based inside demolition. Eskişehir Technical University Journal of Science and Technology B- Theoritical Sciences, 6, 47-56.
- Plummer H (1940). Elements of ordnance. Nature, 145(3673), 443-444. TDIPC (2021). Turkish Defense Industry Product Catalogue. https://www.ssb.gov.tr/urunkatalog/tr/523
- TS 11019 (2015). Procedure to determine the degree of ballistic performance similarity of indirect fire ammunition and applicable corrections to aiming data. Turkish Standards Institution, Ankara, Turkey.
- TS EN 771-4:2011+A1 (2015). Specification for masonry units Part 4: Autoclaved aerated concrete masonry units. Turkish Standards Institution, Ankara, Turkey.
- TS EN 1063 (2002). Glass in building Security glazing Testing and classification of resistance against bullet attack. Turkish Standards Institution, Ankara, Turkey.
- TSE EN 12004-1 (2017). Adhesives for ceramic tiles Part 1: Requirements, assessment and verification of constancy of performance, classification and marking. Turkish Standards Institution, Ankara, Turkey.
- Verhagen A (1978). Impact testing of fibre reinforced concrete: reflection on possible test methods. In: Testing and Test Methods of Fibre Cement Composites. RILEM Symposium Edited by RN Swamy, The Construction Press Ltd., Hornby, 99-105.
- Wikipedia (2021). https://tr.wikipedia.org/wiki/M%C4%B1s%C4%B1r_ni%C5%9Fastas%C4%B1



Research Article

Effects of dry particle coating with nano- and microparticles on early compressive strength of portland cement pastes

Hediye Yorulmaz ^{a,b,*} , Sümeyye Özuzun ^b , Burak Uzal ^a , Serhan İlkentapar ^c , Uğur Durak ^c , Okan Karahan ^{c,d} , Cengiz Duran Atiş ^c

ABSTRACT

It is known that nano-and microparticles have been very popular in recent years since their advantages. However, due to the very small size of such materials, they have very high tendency to agglomeration particularly for nanoparticles. Therefore, it is critical that they are properly distributed in the system to which they are added. This paper investigated the effects of dry particle coating with nano-and microparticles to solve the agglomeration problem. For a clear evaluation, paste samples were preferred to detemine the compressive strength. Nano-SiO2 and nano-CaCO3, micro-CaCO₃ and micro-SiO₂, also known as silica fume, were selected as particulate additives. It was studied by the addition of various percentages (0.3, 0.7, 1, 2, 3 and 5%) of nano-and microparticles in cementitious systems, replacing cement by weight with and without dry particle coating. Dry particle coating was made by using a highspeed paddle mixer. Portland cement and additive particles were mixed at 1500 rpm for 30 seconds in high-speed powder mixer designed for this purpose. The 3-day compressive strength of the cement-based samples to which particles were added at the specified rates was determined and the effect of the dry particle coating on the early strength was investigated. According to the results, it was observed that the production of paste with the dry particle coating technique gave higher compressive strength compared to the production of paste directly in early period. Especially with dry particle coating, compressive strength increased more than 100% in paste samples containing 0.3% nano-SiO₂ compared to direct addition without coating.

ARTICLE INFO

Article history:
Received 5 August 2021
Accepted 24 September 2021

Keywords: Nanoparticle Microparticle Dry particle coating Cementitious paste

1. Introduction

Cement, which is the main component of concrete, is commonly used in the civil engineering area due to its advantages such as high compressive strength, simple preparation, economical and ease to use (Han et al., 2017). On the other hand, Portland cement is a material with high environmental effect due to high amount of CO_2 released to nature and high energy consumption during production of cement (Ouyang et al., 2017). The carbon emission released to the nature during Portland

cement production constitutes approximately 8% of the CO_2 emission in the World (Atiş et al., 2015; Durak et al., 2021) Due to this negative effect of Portland cement, new systems were investigated.

To obtain an eco-friendly system, some amount of cement can be replaced with supplementary cementitious materials like fly ash and silica fume (Camiletti et al., 2013). The use of mineral additives such as micro silica, also known as silica fume, in cementitious systems has positive effects both environmentally and economically, as well as filling voids and showing partial binding effect

^a Department of Civil Engineering, Abdullah Gül University, 38080 Kayseri, Turkey

^b Graduate School of Natural and Applied Sciences, Erciyes University, 38280 Kayseri, Turkey

^c Department of Civil Engineering, Erciyes University, 38280 Kayseri, Turkey

^d Department of Civil Engineering, Kayseri University, 38280 Kayseri, Turkey

(Oltulu and Şahin, 2013). It has been reported that micro- $CaCO_3$ acts as an inert filler and forms a denser microstructure and reduce the setting time (Camiletti et al., 2013).

Nanotechnology can be defined as an emerging research area with potential impact on every field of science and technology (Singh et al., 2013). Nanoparticles have a size between 10 to 1000 nanometers (Mohanraj and Chen, 2007).

According to the literature, nano-SiO₂ and nano-CaCO₃ can enhance the early strength of cementitious systems. In addition, nano-CaCO₃ has been used by many scientists to develop the pore structure and early strength of cementitious systems (Meng et al., 2017; Ren et al., 2021). Besides, it was observed that as the nano-CaCO₃ content increased, the flowability of the system decreased and it has been reported that increasing nano-CaCO₃ content up to a certain value increases the compressive strength (Liu et al., 2012).

Nano-SiO₂, one of the most studied nanoparticles, has three major effects in cementitious materials. These are the filling effect, nucleation effect and pozzolanic effect (Ren et al., 2021). Xu et al. (2016) reported that the inclusion of nano-SiO₂ can optimize the pore structure and accelerate the early hydration. Nano-SiO₂ reacts with calcium hydroxide, which is formed during the cement hydration and does not contribute much to strength development, and additional C–S–H is produced (Singh et al., 2013).

The surface area to volume ratio of nanoparticles is quite high. Nanoparticles with a diameter of 4 nm are very reactive because they have more than half of their atoms on their surface. Chemical reactions at the interface and the agglomeration tendency of materials are key factors to influencing their behavior. This agglomeration affects the rheological properties of systems including nanomaterials that are more difficult to disperse (Senff et al., 2012). In order to observe positive proper-

ties of nanoparticles, particles must be dispersed without agglomeration (Tsuzuki and McCormick, 2004). Cementitious materials containing well-dispersed nanoparticles form dense microstructure, but if the nanoparticles are not properly dispersed, it can cause voids and weak zone formation (Li et al., 2004).

In this study, the effect of dry particle coating on early age of cement-based materials containing micro and nano-sized SiO_2 and $CaCO_3$ were investigated. It is aimed to overcome this agglomeration problem with the dry particle coating.

Compressive strength is a significant property of cementitious materials (Joshaghani et al., 2020). In order to observe the effect of dry particle coating, compressive strength test was performed on the paste samples on the 3rd day and early strength was investigated.

2. Materials and Method

The ordinary Portland cement (CEM I 42.5R) is used for the cement based pastes investigated in this study. In this research, as a particle to be used in cementitious based paste samples; nano calcite (NC), nano silica (NS), micro calcite (MC) and micro silica (MS) have been selected. Their chemical compositions are presented in Table 1.

Nano and micro sized particles were added to the cementitious system in various percentages (0.3, 0.7, 1, 2, 3 and 5%) by replacing the cement weight. But, the surface area of NS is much higher than other particles, hence the maximum dose was determined as 2% for NS. While applying the dry particle coating, cement and particles were mixed in the high speed paddle mixer which

ticles were mixed in the high speed paddle mixer, which is shown in Fig. 1, at 1500 rpm for 30 seconds. As a result of the preliminary studies, 30 seconds was found to be the optimum time for dry particle coating. Longer mixing was not preferred due to the possibility of having a grinding effect on cement particles.

	SiO ₂	Al ₂ O ₃	Fe ₂ O ₃	Ca0	SO ₃	Na ₂ O	K ₂ O	MgO	P ₂ O ₅	TiO ₂	CO ₂	LOI
Cement (PC)	19.18	4.92	3.35	61.50	3.09	0.25	0.55	2.80	-	-	-	3.58
NC*	0.54	0.1	0.01	99.03	-	-	-	0.30	-	-	-	-
NS	99.48	0.1	0.03	0.11	-	0.04	0.02	-	0.03	0.05	-	0.12
MC	0.05	0.15	0.06	55.4	-	-		0.68	-	-	41.2	0.18
MS	93.80	0.21	0.65	0.95	0.41	0.74	1.18	1.02	0.09	-	-	0.13

Table 1. Chemical composition of materials.

*After ignition

The paste mixtures that have been prepared were made into 21x21x21 mm molds. The water/binder ratio was used with a constant value of 0.40 for all paste samples. The paste mixing procedure given in the same standard was followed. Firstly, water was added to the binder material and it was waited for 30 seconds to be fully absorbed. Then, mixing at the low speed for 30 s. After his step, the mixer was stopped and the mortar was allowed to stand for 15 s. Finally, it was mixed at high

speed for a further 60 s. For better compaction of the paste samples, two layers were cast into the molds and after each casting, they were tamped 25 times with a syringe needle. The climate cabinet was set at 99% humidity and 22°C and the samples were cured here for 3 days. The samples taken out of the climate cabinet after 3days are shown in Fig. 2. The paste samples prepared for compressive strength test by removing from the mold with the utility knife are shown in Fig. 3. A universal testing

machine was used to determine the compressive strength of the pastes. Loading speed of 0.2 kN/s was selected for the compressive strength testing. Compressive strength tests were performed on three samples from each mixture and the average values were taken as a result.

3. Results and Discussion

The compressive strength of the samples was tested at the 3 days. The compressive strength of the samples increased with the dry particle coating. The 3-day compressive strength of Portland cement paste was found to be 20.5 MPa. Figs. 4-7 illustrated the 3-day compressive strength of paste samples with and without dry particle coating.



Fig. 1. High-speed paddle mixer.



Fig. 2. Paste samples removed from the climate cabinet after 3 days.



Fig. 3. Samples taken out from the molds and made ready for the experiment.

Fig. 4 shows that the compressive strength of coated paste samples with 0.3, 0.7, 1, 2, 3 and 5% micro-CaCO3 (MC-C) have 20, 17, 19, 34, 18 and 3% higher at early age (3 day) compared to uncoated samples (MC), respectively. According to these results, the sample which the dry particle coating has the most significant effect is 2% MC-C. In addition, the highest strength was obtained from paste made with 2% MC-C which is 30.6 MPa.

Fig. 5 illustrates that the compressive strength of coated specimens with the addition of MS percentage as 0.3, 0.7, 1, 2, 3 and 5% are 16, 10, 11, 11, 1 and 7% higher, respectively, than uncoated samples. This results imply

that the dry particle coating has a little positive effect on the compressive strength of cement-based materials with MS. The reason for this situation may be that the dry particle coating is not applied very well on the samples with MS added.

Based on Fig. 6, the application of dry particle coating significantly increased the strength gain early age for 2%NC-C samples. The addition of 2% NC with dry particle coating improved the compressive strength of the paste by more than 40% compared to the uncoated sample. Fig. 7 demonstrates that the compressive strength of coated specimens with the incorporation of NS percentage as 0.3, 0.7, 1 and 2% are 113, 8, 1 and 26% higher,

respectively, compared to uncoated samples. The effect of the dry particle coating is remarkable for cementitious materials with 0.3% NS. The compressive strength val-

ues for the coated cementitious material with 0.3% NS (NS-C) is 32 MPa while uncoated cement-based material with 0.3% NS is 15 MPa.

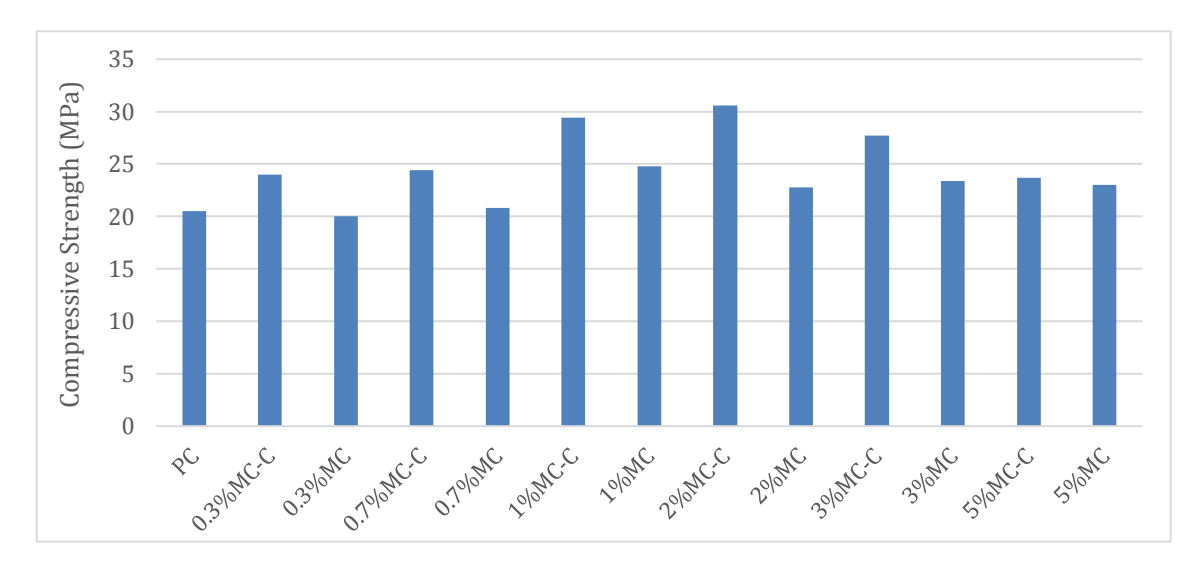


Fig. 4. 3-day compressive strength of pastes with coated and uncoated systems containing MC.

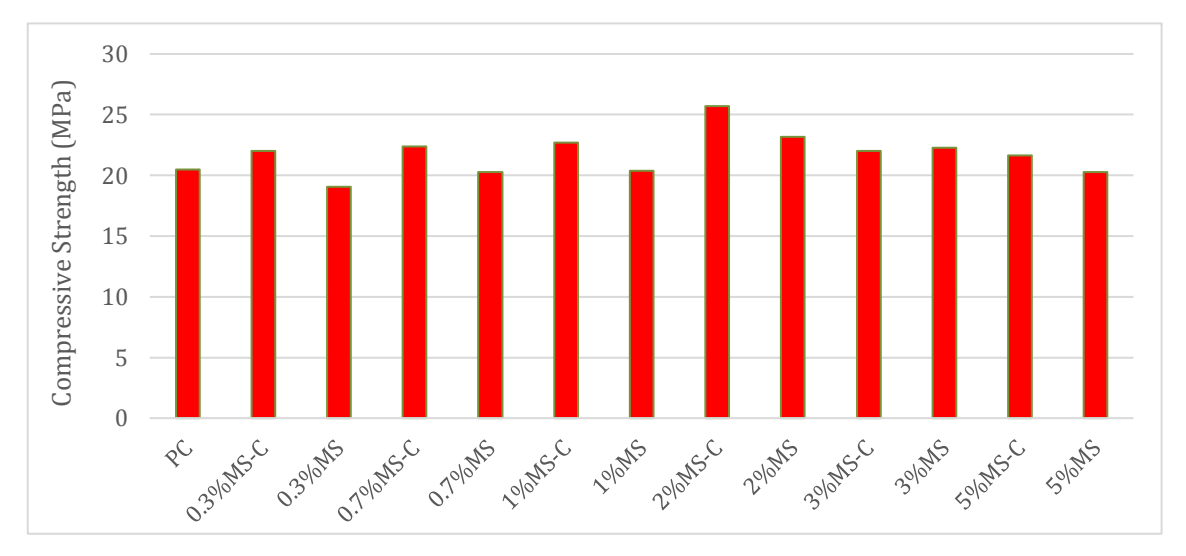


Fig. 5. 3-day compressive strength of pastes with coated and uncoated systems containing MS.

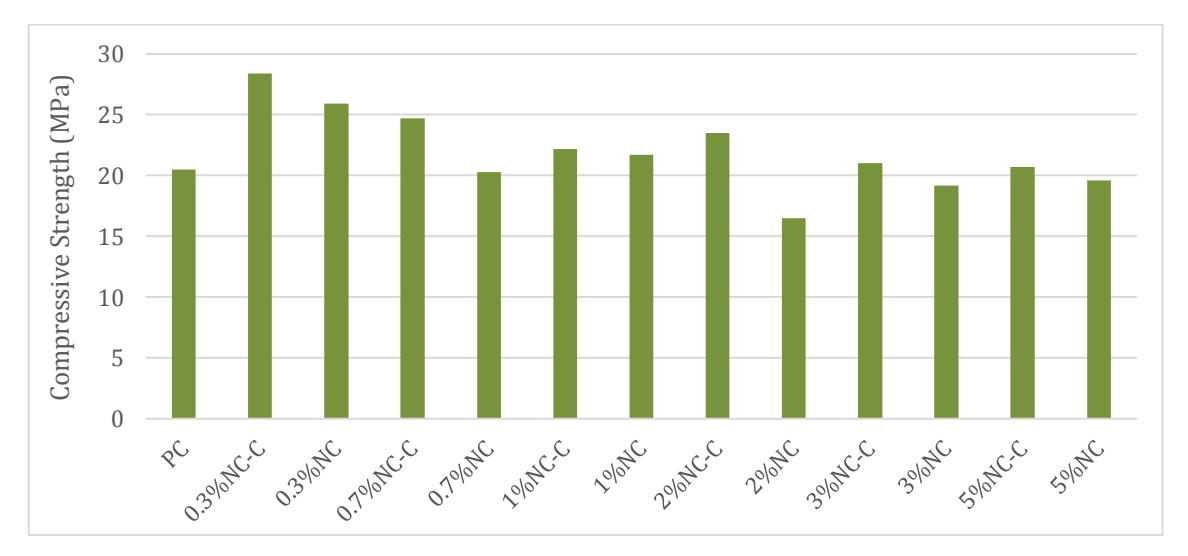


Fig. 6. 3-day compressive strength of pastes with coated and uncoated systems containing NC.

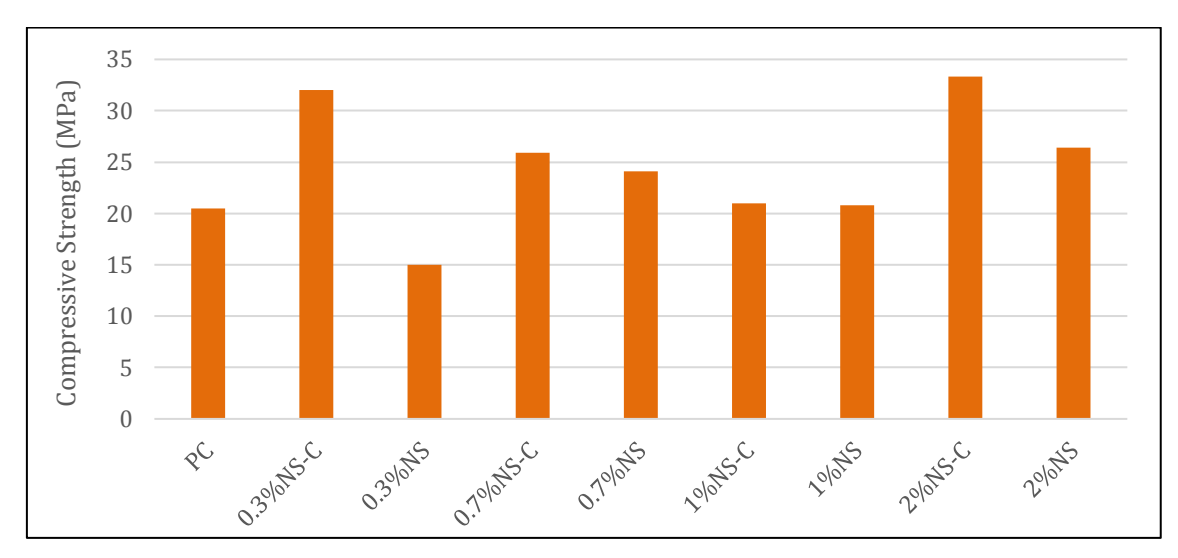


Figure 7. 3-day compressive strength of pastes with coated and uncoated systems containing NS.

4. Conclusions

In this publication, the dry particle coating on cement-based materials with the addition of micro-and nano sized SiO_2 and $CaCO_3$ was investigated. The following conclusions can be made from the results of this research:

- Experimental results indicate that the cementitious system with the addition of 0.3% NS has the highest effect on the compressive strength of the dry particle coating among all paste mixtures.
- Dry particle coating has not a significant effect on the compressive strength of cementitious materials incorporating with MS.
- Among the samples containing NC, the dry particle coating improved the compressive strength of the sample which is containing 2% NC by 42%.
- The most significant effect of the dry particle coating on the MC added samples was observed at 2% MC.
 34% increase in compressive strength was observed in the coated 2% MC compared to the uncoated samples.
- It has been observed that dry particle coating has a
 positive effect on the mixtures prepared by adding
 nano and micro scale calcite and silica to cementitious
 systems.

More studies can be conducted on the effect of dry particle coating on the mechanical and physical properties of systems containing nanoparticles in the later stage in future.

Publication Note

This research has previously been presented at the International Congress on Art and Design Research and Exhibition held in Niğde, Turkey, on June 21-22, 2021. Extended version of the research has been submitted to Challenge Journal of Concrete Research Letters and has been peer-reviewed prior to the publication.

REFERENCES

Atiş CD, Görür EB, Karahan O, Bilim C, Ilkentapar S, Luga E (2015). Very high strength (120 MPa) class F fly ash geopolymer mortar activated at different NaOH amount, heat curing temperature and heat curing duration. *Construction and Building Materials*, 96, 673–678.

Camiletti J, Soliman AM, Nehdi ML (2013). Effects of nano- and microlimestone addition on early-age properties of ultra-high-performance concrete. *Materials and Structures*, 46(6), 881–898.

Durak U, Karahan O, Uzal B, İlkentapar S, Atiş CD (2021). Influence of nano SiO2 and nano CaCO3 particles on strength, workability, and microstructural properties of fly ash-based geopolymer. *Structural Concrete*, 22(S1), 352–367.

Han B, Li Z, Zhang L, Zeng S, Yu X, Han B, Ou J (2017). Reactive powder concrete reinforced with nano SiO2-coated TiO2. Construction and Building Materials, 148, 104–112.

Joshaghani A, Balapour M, Mashhadian M, Ozbakkaloglu T (2020). Effects of nano-TiO2, nano-Al2O3, and nano-Fe2O3 on rheology, mechanical and durability properties of self-consolidating concrete (SCC): An experimental study. Construction and Building Materials, 245, 118444.

Li H, Xiao HG, Yuan J, Ou J (2004). Microstructure of cement mortar with nano-particles. *Composites Part B: Engineering*, 35(2), 185–189.

Liu X, Chen L, Liu A, Wang X (2012). Effect of nano-CaCO3 on properties of cement paste. *Energy Procedia*, 16(Part B), 991–996.

Meng T, Qiang Y, Hu A, Xu C, Lin L (2017). Effect of compound nano-CaCO3 addition on strength development and microstructure of cement-stabilized soil in the marine environment. *Construction and Building Materials*, 151, 775–781.

Mohanraj VJ, Chen Y (2007). Nanoparticles - A review. *Tropical Journal of Pharmaceutical Research*, 5(1), 561–573.

Oltulu M, Şahin R (2013). Effect of nano-SiO2, nano-Al2O3 and nano-Fe2O3 powders on compressive strengths and capillary water absorption of cement mortar containing fly ash: A comparative study. *Energy and Buildings*, 58, 292–301.

Ouyang X, Koleva DA, Ye G, van Breugel K (2017). Insights into the mechanisms of nucleation and growth of C–S–H on fillers. *Materials and Structures*, 50(5), 1–13.

Ren Z, Liu Y, Yuan L, Luan C, Wang J, Cheng X, Zhou Z (2021). Optimizing the content of nano-SiO2, nano-TiO2 and nano-CaCO3 in Portland cement paste by response surface methodology. *Journal of Building Engineering*, 35, 102073.

Senff L, Hotza D, Lucas S, Ferreira VM, Labrincha JA (2012). Effect of nano-SiO2 and nano-TiO2 addition on the rheological behavior and the hardened properties of cement mortars. *Materials Science and Engineering A*, 532, 354–361.

- Singh LP, Karade SR, Bhattacharyya SK, Yousuf MM, Ahalawat S (2013).

 Beneficial role of nanosilica in cement based materials A review.

 Construction and Building Materials, 47, 1069-1077.
- $Tsuzuki\ T, McCormick\ PG\ (2004).\ Mechanochemical\ synthesis\ of\ nanoparticles. {\it Journal\ of\ Materials\ Science,\ } 39(16-17), 5143-5146.$
- Xu Z, Zhou Z, Du P, Cheng X (2016). Effects of nano-silica on hydration properties of tricalcium silicate. *Construction and Building Materials*, 125, 1169–1177.



Research Article

Strength properties of biopolymer treated clay/marble powder mixtures

Zeynep Nese Kurt Albayrak a,* 🕞, Banu Altun a 🕞

^a Department of Civil Engineering, Atatürk University, 25240 Erzurum, Turkey

ABSTRACT

Depending on their unique layer structures and chemical structures, soil problems such as swelling, settlement and loss of strength can be seen especially on clay soils when exposed to water. Settlement occurring on clay soils on which the structure is built, causes various damages in the building. Additionally, in the clay soil interacting with water, strength loss occurs due to the effect of the building load. Today, when soil improvement techniques are developed and diversified, clay soils can be stabilized by using different additives. A clay soil that has been improved by adding waste marble powder within the scope of this study in certain percentages (5%, 15%, 25%), biopolymer added clay / marble powder samples were obtained by interacting with locust bean gum in certain percentages (0.5%, 1%, 1.5%). There are many studies in the literature on improving clay soils using only marble powder or only biopolymer. In this study, marble powder and biopolymer were used together and thus, the feasibility of a more effective soil improvement has been investigated. The results showed that the unconfined compressive strength of the biopolymer added clay-marble powder mixtures are higher when compared with natural clay. Similarly, shear box test results showed that the unconsolidated-undrained cohesions and internal friction angles of the doped clay samples increased. It was observed that the strength values of marble powder-added clay increased after improving with biopolymer.

ARTICLE INFO

Article history: Received 28 July 2021 Revised 13 September 2021 Accepted 2 October 2021

Keywords: Biopolymer Clay Soil stabilization Strength

1. Introduction

Clayey soils are problematic soils because of the swelling and / or settlement behaviors. For eliminating this problems, clayey soils can be stabilize with additives. These additives can be industrial wastes such as marble powder, fly ash, silica fume and red mud (Çokça, 2001; Senol et al., 2006; Hossain and Mol, 2011; Edil et al., 2006; Yarbaşı et al., 2007; Brooks, 2009; İkizler et al., 2014). In addition to these, chemical additives and various polymers are also used in stabilization of clay soils (Tingle and Santoni, 2003; Akbulut et al., 2012; Akbulut et al., 2013).

Marble is a metamorphic rock formed by the metamorphism of limestone and dolomitic limestone. When marble blocks are cut to give a smooth geometric shape, high volumes of marble waste are produced (Hebhoub et

al., 2011). During the cutting process, water is used to prevent the cutting tip from overheating and dust generation. During the cutting of marbles, the mixture of water and marble powder comes out as a slurry. Turkey has approximately 5.2 billion cubic meters of marble reserves and, considering that about 30-40% of a marble block is generated as waste in the cutting process, it can be said that about 2.5 million tons of marble mud in marble production has emerged as waste in Turkey (Alyamaç and Aydın, 2015). The effects of waste marbles on the engineering and geotechnical properties of clay soils have been investigated in the literature (Gurbuz, 2015; Jain and Jha, 2020; Sivrikaya et al., 2020).

Biopolymers are organic polymers. Biopolymers are produced by biological organisms and easily found in nature (Ashraf et al., 2017). Soil improvement with using biopolymers is one of the soil improvement methods

that do not harm the environment (Chang et al., 2019). The use of low ratios of biopolymer can increased the soil strength (Chang and Cho, 2019). There are many studies that use biopolymers to improve the strength properties of soils (Khatami and O'Kelly, 2013; Smitha and Sachan, 2016; Viswanath et al., 2017). In studies where biopolymers are used in soil improvement, usually xanthan gum (Lee et al., 2017, Lee et al., 2019, Singh and Das, 2020), guar gum (Ayeldeen et al., 2016; Latifi et al., 2016; Sujatha and Saisree, 2019) and gellan gum (Chang et al., 2016a; Im et al., 2017; Chang and Cho, 2019) are used. Swelling properties (Singh and Das, 2020) and permeability properties of soils (Wiszniewski and Cabalar, 2014), can be improved with biopolymers. The geotechnical properties of clay soils can be improved with deep mixing using biopolymers (Arasan et al., 2017). In the production of nanoclay-composites, biopolymers are used to increase gel strength (Maier et al., 1993). Another biopolymer used in soil improvement is locust bean gum. It has been observed that the nanoclaycomposites obtained by using locust bean gum have improved geotechnical properties when compared with natural clay (Kurt and Akbulut, 2014; Kurt and Akbulut, 2017; Majedi et al., 2019; Kurt Albayrak and Gencer, 2021). Locust bean gum is also called carob gum (Lopes da Silva et al., 1994). Locust bean gum has a non-ionic structure, and it is not affected by heat, pH and salt (Barak and Mudgil, 2014).

Within the scope of this study, marble powder which is a waste material and used in soil improvement, was added to a clay soil and, clay soils with marble powder were obtained. In the continuation of the study, marble powder-added clay soils were interacted with locust bean gum and, it has been investigated that how the biopolymer changes the strength properties of marble powder-added clay samples. There are many studies on improving clay soils using only marble powder or biopolymer. In this study, marble powder and biopolymer were used together and thus, the feasibility of a more effective soil improvement was investigated. For this purpose, a natural clay belonging to Erzurum Oltu region was mixed with marble powder in certain ratios obtained from Pazaryolu-Erzurum. Then, marble powder added clays were improved with locust bean gum in certain ratios and biopolymer added clay / marble powder samples were obtained. The experimental results of the samples obtained, were compared with the results of natural clay samples.

2. Materials and Method

2.1. Clay

The clay (C) sample from Erzurum (Oltu-Narman) environment was used in this study. The clay content of natural clay (<0.002 mm) is 42% and its specific gravity is 2.64. In the classification made according to the Unified Soil Classification System (USCS), it was seen that, it is CH (high plasticity clay). Some geotechnical properties of natural clay are given in Table 1 and the results of X-ray fluorescence spectrometry (XRF) analysis of the clay sample, are given in Table 2.

Table 1. Clay properties.

Properties	Clay
Liquid limit, %	70
Plastic limit, %	27
Plasticity index, %	43
Optimum moisture content, %	26
Maximum dry unit weight, kN/m ³	15.2

Table 2. Chemical compounds of clay and marble.

Content	Clay, %	Marble, %
SiO ₂	59.3	2.5
Al_2O_3	16.5	0.4
CaO	1.50	54.0
Fe_2O_3	8.0	0.3
K ₂ O	1.6	<0.1
MgO	2.1	0.5
MnO	<0.1	<0.1
Na ₂ O	1.4	0.1
P ₂ O ₅	0.2	<0.1
TiO ₂	0.6	<0.1
LOI	8.5	42.05

2.2. Marble powder

Waste marble powder (M) used in the experiments was obtained from Erzurum's Pazaryolu district. In the experiments, marble powder was used by sieving it through a No. 40 sieve (sieve diameter: 0.425 mm). The specific gravity of the marble powder was 2.85. XRF analysis results of the marble powder, are shown in Table 2.

2.3. Biopolymer (locust bean gum)

The chemical content of the locust bean gum (L) is a type of hydrocolloids, Galactomannan, its pH is between 5-7, and its viscosity is between 2000-3500 cps (Kurt and Akbulut, 2014; Kurt Albayrak and Gencer, 2021). Locust bean gum, is a biopolymer and obtained from the carob tree (Cerationia saiqua) of legume group, has a thickener, gelling and stabilizing properties (Dey et al., 2012).

2.4. Specimen preparation

Marble powder-added clay samples were derived by mixing clay with certain percentages of marble powder (5%, 15%, 25%) in dry form. While obtaining samples with biopolymer additives, locust bean gum was mixed with distilled water in a mechanical stirrer until dissolved at 1000 rpm and, by calculating the percentage of water used in the experiments (0.5%, 1%, 1.5%), clay and marble powder-added clay samples were added together with water. The samples prepared, are shown in Table 3.

Table 3. Samples.

Sample	Clay	Marble powder	Locust bean gum	
C-%0 L	100	-	-	
C-%0.5L	100	-	0.5	
C-%1L	100	-	1	
C-%1.5L	100	-	1.5	
C-%5M-%0L	95	5	-	
C-%5M-%0.5L	95	5	0.5	
C-%5M-%1L	95	5	1	
C-%5M-%1.5L	95	5	1.5	
C-%15M-%0L	85	15	-	
C-%15M-%0.5L	85	15	0.5	
C-%15M-%1L	85	15	1	
C-%15M-%1.5L	85	15	1.5	
C-%25M-%0L	75	25	-	
C-%25M-%0.5L	75	25	0.5	
C-%25M-%1L	75	25	1	
C-%25M-%1.5L	75	25	1.5	

2.5. Tests

Direct shear box and unconfined compressive strength tests were carried out on clay samples, marble powder added clay samples and biopolymer added samples obtained by improving them with locust bean gum. Unconfined compression tests were performed on the basis of ASTM D 2166. The unconfined compression tests were conducted on the cylindrical samples (diameter is 35mm, height is 70 mm) compacted at optimum moisture content at standard proctor energy. The optimum moisture content and maximum dry unit weight values of the samples determined by the standard proctor test are, shown in Table 4 (Kurt Albayrak and Altun, 2018).

Direct shear box tests were carried out according to ASTM D 3080. Shear box experiments were carried out on samples placed in 6 cm diameter shear box from compaction samples prepared by optimum moisture content.

3. Results and Discussion

3.1. Unconfined compression test results

The unconfined compressive strengths obtained as a result of the unconfined compression test carried out, are given in Table 5. The change in the unconfined compressive strength of the samples with the increase in the ratio of locust bean gum, is seen in Fig. 1.

When Fig. 1 is examined, it is observed that when the locust bean gum percentage is increased, the unconfined compressive strength of clay and marble powder added clay also increases. According to Fig. 1, the unconfined compressive strength of clay, increased by 46%, 54% and 136%, when the biopolymer percentage is 0.5%, 1%, 1.5% respectively. Due to the fact that biopolymers can

interact effectively with fine grained soils, it can be thought that the unconfined compression strength increases with the increase in the percentage of locust bean gum (Chang et al., 2015). Biopolymer-soil matrices with high strength are formed, with the ability of biopolymers that can interact with fine-grained soils due to their large electrically charged surface area (Chang et al., 2016b). Chen et al. (2013) similarly stated that, bond structures are formed between biopolymer and soil particles and, this increased the strength.

Table 4. Compaction parameters of samples.

•	•	•
	Optimum	Maximum dry
Sample	moisture	unit weight,
	content, %	kN/m³
C-%0 L	26	15.2
C-%0.5L	23	14.4
C-%1L	22.5	14.3
C-%1.5L	22	14.7
C-%5M-%0L	23.9	15.2
C-%5M-%0.5L	19.5	14.8
C-%5M-%1L	22.5	14.7
C-%5M-%1.5L	19	15.3
C-%15M-%0L	22.2	15.3
C-%15M-%0.5L	22	15.1
C-%15M-%1L	24	15.1
C-%15M-%1.5L	19.5	15.5
C-%25M-%0L	23	15.4
C-%25M-%0.5L	19.5	15.4
C-%25M-%1L	21.4	15.4
C-%25M-%1.5L	18	15.7

Table 5. Unconfined compression test results of samples.

Sample Unconfined compressi strength, kPa		
C-%0 L	156	
C-%0.5L	228	
C-%1L	240	
C-%1.5L	369	
C-%5M-%0L	177	
C-%5M-%0.5L	245	
C-%5M-%1L	260	
C-%5M-%1.5L	370	
C-%15M-%0L	240	
C-%15M-%0.5L	260	
C-%15M-%1L	269	
C-%15M-%1.5L	378	
C-%25M-%0L	255	
C-%25M-%0.5L	288	
C-%25M-%1L	300	
C-%25M-%1.5L	404	

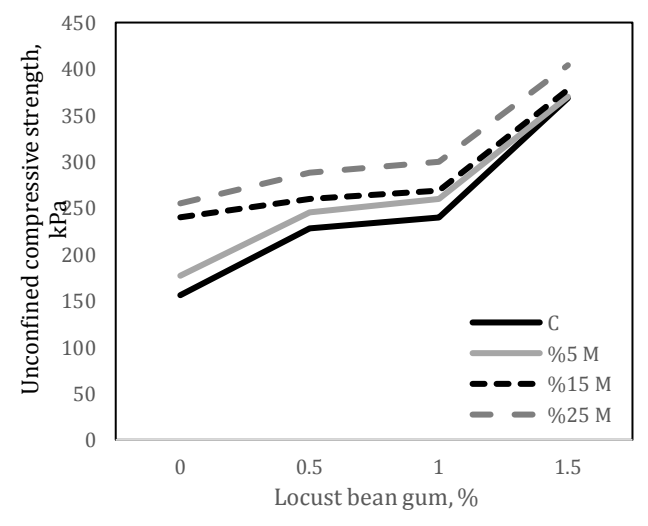


Fig. 1. Change in unconfined compressive strength with locust bean gum.

By comparing the unconfined compression strength of the samples obtained by adding locust bean gum solution to clay samples with 5% marble powder added with the unconfined compressive strength of natural clay, the biopolymer percentage increased by 57%, 67% and 137% for 0.5%, 1%, 1.5%, respectively. By comparing the unconfined compression strength of the samples obtained by adding locust bean gum solution to 15% marble powder added clay samples with the unconfined compression strength of natural clay, the biopolymer percentage increased by 67%, 72% and 142% for 0.5%, 1%, 1.5%, respectively. By comparing unconfined compression strength of the samples obtained by adding locust bean gum solution to 25% marble powder added clay samples with the unconfined compression strength of natural clay, the biopolymer percentage increased by 85%, 92% and 159% for 0.5%, 1%, 1.5%, respectively.

In addition, the increase in marble additive, generally increased the unconfined compression strength of biopolymer added clay samples. It is seen that locust bean gum additive increases the unconfined compression strength of natural clay and marble powder added clay samples.

3.2. Direct shear box tests

The experimental results obtained as a result of the direct shear box tests performed are given in Table 6. The change in unconsolidated-undrained cohesion and internal friction angle with the increase in locust bean gum percentage, is given in Figs. 2 and 3, respectively.

Table 6. The direct shear box test results of samples

Sample	Unconsolidated undrained cohesion, kPa	Internal friction angle, °
C-%0 L	174	7.7
C-%0.5L	312	7.9
C-%1L	312	8.0
C-%1.5L	312	9.5
C-%5M-%0L	101	7.9
C-%5M-%0.5L	295	8.0
C-%5M-%1L	296	8.2
C-%5M-%1.5L	302	10.4
C-%15M-%0L	100	12.4
C-%15M-%0.5L	260	12.8
C-%15M-%1L	273	17.0
C-%15M-%1.5L	282	18.0
C-%25M-%0L	99	13.0
C-%25M-%0.5L	251	15.0
C-%25M-%1L	266	18.2
C-%25M-%1.5L	272	18.4

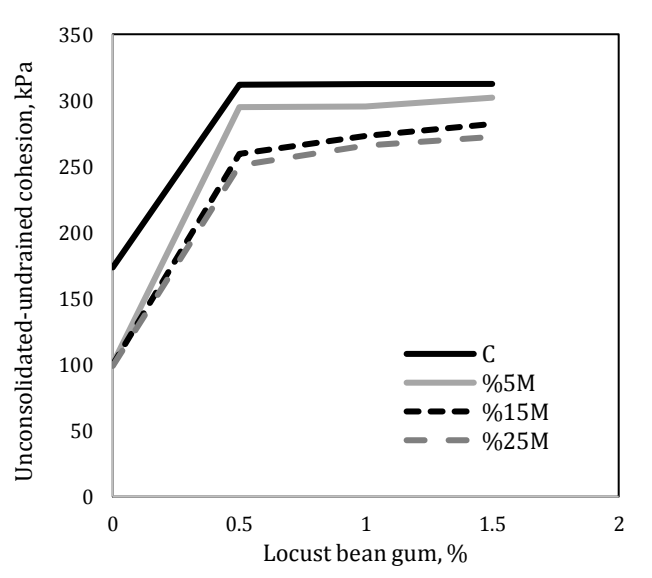


Fig. 2. Change in unconsolidated-undrained cohesion values of samples.

When Fig. 2 is examined, it is observed that as the percentage of marble increases, unconsolidated-undrained cohesion of natural clay decreases. The cohesion values of 0.5%, 1%, 1.5% locust bean gum added 5% marble powder/clay samples increased by 70%, 70.3% and 74% respectively according to the cohesion values of natural clay. The cohesion values of 0.5%, 1%, 1.5% locust bean gum added 15% marble powder/clay samples increased by 50%, 57% and 62% respectively according to the cohesion values of natural clay. Similarly, the cohesion values of 0.5%, 1%, 1.5% locust bean gum added 25% marble powder/clay samples increased by 44%, 53% and 56% respectively according to the cohesion values of natural clay.

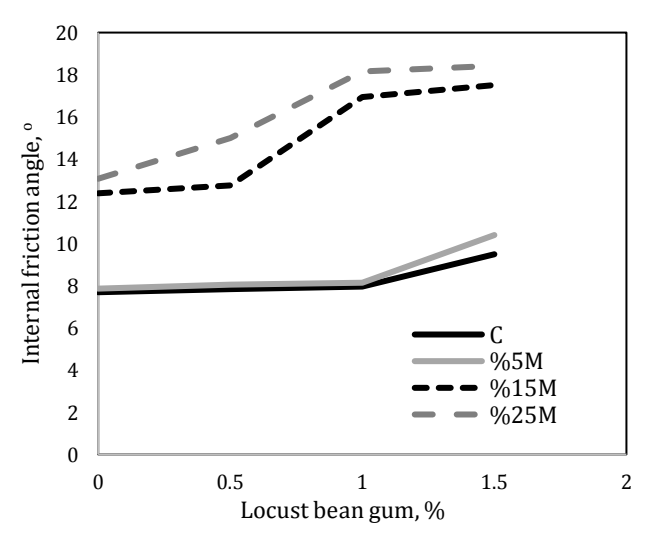


Fig. 3. Change in internal friction angle values of samples.

According to Fig. 3, as the percentage of marble powder increased, the internal friction angle of natural clay increased partially. In addition, it is seen that the value of the internal friction angle of natural clay increased by 2%, 3.5%, 23.4% respectively for the locust bean gum percentage of 0.5%, 1%, 1.5%.

The internal friction angle values of natural clay increased by 4.5%, 6% and 35%, when compared with the internal friction angle values of the 0.5%, 1%, 1.5% locust bean gum solution added 5% marble powder/clay samples, respectively. According to the internal friction angle values of natural clay of the internal friction angle values of the samples obtained by adding 0.5%, 1%, 1.5% locust bean gum solution to 15% marble powder/clay samples, increased by 66%, 120%, 128% respectively. According to the internal friction angle values of natural clay of the internal friction angle values of the samples obtained by adding 0.5%, 1%, 1.5% locust bean gum solution to 25% marble powder/clay samples, increased by 95%, 136%, and 140% respectively.

It is seen that the biopolymer additive generally increases the internal friction angle and cohesion. The direct shear box test results showed that the biopolymer additive increased the cohesion in natural clay, while the increase in the biopolymer percentage did not change the cohesion significantly. The internal friction angle increased with the increase in the biopolymer percentage.

Significant increases in both cohesion and internal friction angle occurred with the increase in the ratio of biopolymer in marble powder added clays.

The change in internal friction angle and cohesion, changes according to the soil type, grain diameter and type of biopolymer (Soldo et al., 2020). Due to the increased contact between particles in biopolymer treated soils, it is thought that the internal friction angle will increase (Chang et al., 2016b). Soldo and Miletic (2019) stated in their study that the biopolymer of xanthan gum significantly increased the cohesion in cohesionless soils but, they did not change the internal friction angle significantly. They pointed out that this change, is the interaction between the biopolymer and the soil related to the grain size. They stated that the biopolymer forms bonds between distant particles by coating the coarse grains and, that the electrostatic bond occurs with fine-grained soils and that this bond is stronger. It is believed that the strengthening mechanism of biopolymers is the formation of biopolymer-clay soil matrices and the improvement in friction through coarse grains (Chang et al., 2016b). In this study, it can be thought that the increase in the locust bean gum ratio and the increase in the cohesions and internal friction angles of the marble powder-added clays can be result from the formation of biopolymer-clay matrices. Additionally, the increase in friction caused by marble powder could increase the internal friction angle of locust bean gum added samples.

4. Conclusions

Within the scope of the study, the strength properties of the samples obtained as a result of improving the marble powder-added clay samples with the locust bean gum were investigated. For that purpose, a clay belonging to Erzurum-Oltu region was firstly mixed with marble powder obtained from Erzurum-Pazaryolu at certain ratios and as a result, clay with marble powder was obtained. Then, marble powder added clays were treated with locust bean gum in certain ratios and as a result, locust bean gum added clay/marble powder samples were obtained. Direct shear box and unconfined compressive strength tests were performed on the samples. The results obtained, are listed below.

- Unconfined compressive strength of marble powderadded clay samples increased with the increase in the percentage of marble powder.
- As the locust bean gum percentage increased, the unconfined compressive strength of natural clay increased.
- The unconfined compressive strength of locust bean gum added clay / marble powder mixtures increased with locust bean gum percentage.
- The unconsolidated-undrained cohesion values of natural clay samples with added marble powder decreased with the marble powder percentage.
- The internal friction angle of clay increased with marble powder.

- As the locust bean gum percentage increased, the unconsolidated-undrained cohesion value of clay increased.
- With the increase in the percentage of locust bean gum, the internal friction angle of natural clay also increased.
- The unconsolidated-undrained cohesion values of the locust bean gum added clay / marble powder mixtures increased with locust bean gum percentage.
- With the increase in the percentage of locust bean gum, the internal friction angle of the clay/ marble powder samples also increased.

It is known that marble powder is used in the clay soils stabilization. It is clear that the addition of marble powder increases the strength of clay. Additionally, higher strength values were obtained by adding locust bean gum to natural clay as well as marble powder. As a result of the study, it has been shown that the use of an environmentally friendly polymer, locust bean gum together with marble powder which is a waste material, provides a more effective stabilization in the stabilization of clay soils. Additionally, it is thought that with the stabilization of clay soils with marble powder and biopolymer, the damages that may occur due to the foundation soil in the structures to be built on clay soils will be prevented. It is known that other properties such as hydraulic conductivity and swelling pressure change with the change in the strength properties of clays, and in order to better understand the effects of biopolymers on the geotechnical properties of marble powder added clays in the future studies, it is thought that the changes in the internal structure of the samples should also be examined with special analysis methods besides some properties such as swelling pressure, hydraulic conductivity. In addition, due to the degradation of biopolymers over time, their long-term performance should be studied in detail.

REFERENCES

- Akbulut S, Kurt Z, Arasan S (2012). Surfactant modified clays consistency limits and contact angles. *Earth Sciences Research Journal*, 16, 95-101.
- Akbulut S, Kurt Z, Arasan S, Pekdemir Y (2013). Geotechnical properties of some organoclays. Sadhana-Academy Proceedings in Engineering Sciences, 38, 317-329.
- Alyamaç KE, Aydın AB (2015). Concrete properties containing fine aggregate marble powder. KSCE Journal of Civil Engineering, 19(7), 2208-2216.
- Arasan S, Bagherinia M, Akbulut RK, Zaimoglu AS (2017). Utilization of polymers to improve soft clayey soils using the deep mixing method. *Environmental and Engineering Geoscience*, 23(1), 1-12.
- Ashraf MS, Azahar SB, Yusof NZ (2017). Soil improvement using MICP and biopolymers: A review. IOP Conf. Series: Materials Science and Engineering, 226, 012058.
- Ayeldeen MK, Negm AM, El Sawwaf MA (2016). Evaluating the physical characteristics of biopolymer/soil mixtures. *Arabian Journal of Geoscience*, 9, 371.
- Barak S, Mudgil D (2014). Locust bean gum: Processing, properties and food applications-A review. *International J of Biological Macromolecules*, 66, 74-80.

- Brooks RM (2009). Soil stabilization with fly ash and rice husk ash. *International Journal of Research and Reviews in Applied Sciences*, 1(3), 209-217.
- Chang I, Im J, Prasidhi AK, Cho GC (2015). Effects of xanthan gum biopolymer on soil strengthening. Construction and Building Materials, 74, 65-72.
- Chang I, Im J, Cho GC (2016a). Geotechnical engineering behaviors of gellan gum biopolymer treated sand. *Canadian Geotechnical Journal*, 53(10), 1658-1670.
- Chang I, Im, J, Cho GC (2016b). Introduction of microbial biopolymers in soil treatment for future environmentally-friendly and sustainable geotechnical engineering. Sustainability, 8, 251.
- Chang I, Cho GC (2019). Shear strength behavior and parameters of microbial gellan gum treated soils: from sand to clay. *Acta Geotechnica*, 14, 361-375.
- Chang I, Kwon YW, Im J, Cho GC (2019). Soil consistency and interparticle characteristics of xanthan gum biopolymer-containing soils with pore-fluid variation. *Canadian Geotechnical Journal*, 56, 1206-1213
- Chen R, Zhang L, Budhu M (2013). Biopolymer stabilization of mine tailings. *Journal of Geotechnical and Geoenvironmental Engineering*, 139(10), 1802-1807.
- Çokca E (2001). Use of class C fly ashes for the stabilization of an expansive soil. *Journal of Geotechnical and Geoenvironmental Engineering*, 1277, 568-573.
- Dey P, Maiti S, Sa B (2012). Locust bean gum and its application in pharmacy and biotechnology: An overview. *International Journal of Current Pharmaceutical Research*, 4(1), 7-11.
- Edil T, Acosta HA, Benson CH (2006). Stabilizing soft fine grained soils with fly ash. *Journal of Materials in Civil Engineering*, 18(2), 283-294.
- Gurbuz A (2015). Marble powder to stabilise clayey soils in subbases for road construction. *Road Materials and Pavement Design*, 16(2), 481-492.
- Hebhoub H, Aoun H, Belachia M, Houari H, Ghorbel E (2011). Use of waste marble aggregates in concrete. *Construction and Building Materials*, 25, 1167-1171.
- Hossain KMA, Mol L (2011). Some engineering properties of stabilized clayey soils incorporating natural pozzolans and industrial wastes. *Construction and Building Materials*, 25, 3495-3501.
- Im J, Chang I, Cho GC (2017). Small strain stiffness and elastic behavior of gellan treated soils with confinement. Geotechnical Frontiers, Orlando, Florida.
- İkizler SB, Şenol A, Etminan E, Khosrowshahi SK, Hatipoğlu M (2014). Improvement of expansive soils using chemical stabilizers. AGU Fall Meeting 2014, San Francisco, USA.
- Jain AK, Jha AK (2020). Geotechnical behaviour and micro-analyses of expansive soil amended with marble dust. *Soils and Foundations*, 60(4), 737-751.
- Khatami HR, O'Kelly BC (2013). Improving mechanical properties of sand using biopolymers. *Journal of Geotechnical and Geoenvironmental Engineering*, 139(8), 1402-1406.
- Kurt ZN, Akbulut S (2014). The dynamic shear modulus and damping ratio of clay nanocomposites. Clays and Clay Minerals, 62(4), 313-323.
- Kurt ZN, Akbulut S (2017). Some geotechnical properties of clay nanocomposites. *Periodica Polytechnica Civil Engineering*, 61(3), 381-388.
- Kurt Albayrak ZN, Altun B (2018). Investigation of some geotechnical properties of clay/marble mixtures modified with a biopolymer. *Zemin Mekaniği ve Geoteknik Mühendisliği 17. Ulusal Konferansı*, Istanbul, Turkey (in Turkish).
- Kurt Albayrak ZN, Gencer G (2021). The usability of clay/pumice mixtures modified with biopolymer as an impermeable liner. *KSCE Journal of Civil Engineering*, 25(1), 28-36.
- Latifi N, Horpibulsuk S, Meehan CL, Majid MZA, Tahir MM, Mohamad ET (2016). Improvement of problematic soils with biopolymer—An environmentally friendly soil stabilizer. *Journal of Materials in Civil Engineering*, 29(2), 04016204.
- Lee S, Chang I, Chung MK, Kim Y, Kee J (2017). Geotechnical shear behavior of xanthan gum biopolymer treated sand from direct shear testing. *Geomechanics and Engineering*, 12(5), 831-847.

- Lee S, Im J, Cho GC, Chang I (2019). Tri-axial shear behavior of xanthan gum biopolymer-treated sand. ASCE Geo-Congress 2019, Soil Improvement.
- Lopes da Silva JA, Gonçalves MP, Rao MA (1994). Influence of temperature on the dynamic and steady-shear rheology of pectin dispersions. *Carbohydrate Polymers*, 23(2), 77-87.
- Maier M, Anderson M, Karl C, Magnuson K (1993). Industrial Gums Polysaccharides and Their Derivatives. In: Whistley RL, BeMiller JN, editors. Guar, Locust Bean, Tara and Fenugreek Gums. Academic Press, San Diego, California, 205-213.
- Majedi P, Akbulut S, Kurt ZN (2019). Some geotechnical properties and damping ratio of clay nanocomposites. *Journal of Engineering Re*search, 7(1), 1-16.
- Senol A, Edil TB, Bin-Shafique MS, Acosta HA, Benson CH (2006). Soft subgrades' stabilization by using various fly ashes. *Resources, Con*servation and Recycling, 46(4), 365-376.
- Singh, S. P., Das, R (2020). Geo-engineering properties of expansive soil treated with xanthan gum biopolymer. Geomechanics and Geoengineering, 15(2), 107-122.
- Sivrikaya O, Uysal F, Yorulmaz A, Aydin K (2020). The efficiency of waste marble powder in the stabilization of fine-grained soils in terms of volume changes. *Arabian Journal for Science and Engineering*, 45, 8561-8576.
- Smitha S, Sachan A (2016). Use of agar biopolymer to improve the shear strength behavior of Sabarmati sand. *International Journal of Geotechnical Engineering*, 10(4), 387-400.
- Soldo A, Miletic M (2019). Study on shear strength of xanthan gumamended soil. *Sustainability*, 11(21), pp. 6142.
- Soldo A, Miletic M, Auad ML (2020). Biopolymers as a sustainable solution for the enhancement of soil mechanical properties. *Scientific Reports*, 10, 267.
- Sujatha ER, Saisree S (2019). Geotechnical behaviour of guar gumtreated soil. *Soils and Foundations*, 59(6), 2155-2166.
- Tingle JS, Santoni RL (2003). Stabilization of clay soils with nontraditional additives. Transportation Research Record, 1819(1), 72-84.
- Viswanath SM, Booth SJ, Hughes PN, Augarde CE, Perlot C, Bruno AW, Gallipoli D (2017). Mechanical properties of biopolymer-stabilised soil-based construction materials. *Géotechnique Letters*, 7(4), 1-18.
- Wiszniewski M, Cabalar AF (2014). Hydraulic conductivity of a biopolymer treated sand. New Frontiers in Geotechnical Engineering, 243, 19-27.
- Yarbaşı N, Kalkan E, Akbulut S (2007). Modification of the geotechnical properties, as influenced by freeze-thaw, of granular soils with waste additives. *Cold Regions Science and Technology*, 48, 44-54.



Research Article

Predictability of concrete damage level by non-destructive test methods

Boğaçhan Akça a,* , Süleyman Bahadır Keskin b, Aysu Göçügenci b ,

^a Department of Civil Engineering, Muğla Sıtkı Koçman University, 48000 Muğla, Turkey

ABSTRACT

Non-destructive methods have many advantages over traditional test methods, especially since it does not damage the specimen, it can be used multiple times on the same specimen. These advantages also provide a great benefit in terms of following the property development in concrete as the same specimens are used which eliminates the variations related to the specimens. In this study, it is aimed to determine the damage amount of concrete produced with different binders by electrical bulk resistivity, resonance frequency, and ultrasonic pulse velocity methods. Firstly, concretes containing different binders were produced, and along with the mechanical properties, ultrasonic wave velocity, resonance frequency, and electrical resistivity values of the produced concrete were determined at the 7, 28, and 90 days. Besides, the specimens were subjected to gradually increased compressive loads and non-destructive methods were used to estimate the extent of damage on specimens. It was attempted to establish a relationship between the damage on concrete specimens and the results obtained by non-destructive methods. Consequently, the compressive strength, electrical resistivity, ultrasonic pulse velocity and resonance frequency values of all specimens increased with the advancing age. It was concluded that the resonant frequency method is more successful than other methods in estimating the amount of damage in concrete.

ARTICLE INFO

Article history:
Received 23 August 2021
Revised 2 October 2021
Accepted 1 November 2021

Keywords:
Non-destructive testing
Concrete
Damage
Mineral admixtures
Compressive strength

1. Introduction

Considering the wide use of concrete as a construction material, degradation of concrete structures is also a great concern. The extent of concrete damage can be evaluated in many ways. Although taking cores from the existing structures is a common method, in recent years, non-destructive testing methods have been used frequently. As concrete is mainly resistant to compressive forces, the compressive strength and some physical properties of concrete can be estimated by non-destructive testing methods. Non-destructive testing methods can be used to determine the concrete quality in new constructions, as well as to determine the properties of the existing structures (ACI 228.2R-98, 1998). By using non-destructive testing methods, an idea about the parameters such as the absorption capacity of concrete,

modulus of elasticity, compressive strength, moisture content, and electrical resistance of concrete can be obtained (Breysse, 2012).

One of the novel non-destructive techniques on concrete uses bulk electrical resistivity to evaluate the concrete's durability. The electrical resistivity of concrete depends on the concrete's water/cement ratio, mineral and chemical admixtures, age, aggregate type, degree of saturation, and the environmental conditions in which it is cured (Layssi et al., 2015). Since the alternating current is employed in the electrical resistivity test, in order to determine the resistivity, impedance and the phase angle values are collected and transformed to resistance and resistivity afterwards (Layssi et al., 2015). In a study of electrical resistance, concrete mixtures were prepared with 4 different types of cement with varying water/binder ratios while, the amount of cement and aggregate type

were kept constant (Medeiros-Junior et al., 2016). According to this research, it is shown that the electrical resistance of concrete can also be affected by the type of cement (Medeiros-Junior et al., 2016). Besides, parameters that can be obtained from the rapid chloride ion penetration test were shown to be obtained by the electrical resistivity test (Shane et al., 1999). Bearing in mind that the rapid chloride ion penetration test takes quite a long time, the electrical resistance test is more advantageous from the practicality point of view. Moreover, some studies showed that the increase in the compressive strength of concrete causes an increase in the electrical resistivity of concrete (Lübeck et al., 2012; Helal et al., 2015). This is because as the compressive strength of the concrete increases, hydration products fill the voids inside the concrete. In damaged concrete, due to the increase in the size of the voids and the number of voids in the damaged parts of concrete, some changes may occur in the electrical resistivity. In this research, the relationship between the damage amount of concrete prepared with different mineral admixtures and electrical resistivity was tried to be found.

Ultrasonic pulse velocity is a common method to evaluate the concrete properties non-destructively. The quality, homogeneity, void state, crack state and crack depth of the concrete can be determined by using an ultrasonic pulse velocity test (ASTM C597-97, 1997). Ultrasonic pulse velocity can be affected by w/c ratio, the maximum size of coarse aggregates, and cement type (ASTM C597-97, 1997; Trtnik et al., 2009). Properties and types of aggregates can affect the compressive strength as well as the ultrasonic pulse velocity of the concrete specimens (Trtnik et al., 2009).

Qasrawi (2000) researched that concrete strength can be predicted by using NDT methods such as ultrasonic pulse velocity and rebound hammer. Also, Mohammed and Mahmood (2016) conducted a study on how aggregate size affects ultrasonic pulse velocity. In their study, brick fractions were used as coarse aggregate in different sizes, and it was concluded that the ultrasonic pulse velocity increased as the aggregate size increased in concrete.

Ultrasonic pulse velocity alongside with compressive strength is affected by the age and curing period of the concrete specimens as well. Demirboğa et al. (2004) investigated ultrasonic pulse velocity and compressive strength parameters in high-volume mineral admixture concrete. In their study, it was observed that both compressive strength and ultrasonic pulse velocity results increased with advancing age and curing period.

Another non-destructive technique adopted in this study is resonance frequency testing. There are two ways to determine the resonance frequency of the concrete: the forced resonance method and the impact resonance method. In the impact resonance method which is used in this experimental work, the specimen is struck with the impactor, and the specimen response is measured with the accelerometer.

Dynamic modulus of elasticity can be estimated by using the resonance frequency test method (ASTM C215-08, 2008). But the result can be affected by the manufacturing process, mix design, aggregate properties, specimen size,

and curing conditions of the concrete (ASTM C215-08, 2008; Helal et al., 2015). One study shows that the self-healing capability of the concrete specimens which are prepared by different pozzolanic materials such as ground granulated blast furnace slag and Class F fly ash can be determined by using NDT methods such as electrical impedance, rapid chloride permeability test, and resonance frequency (Yildirim et al., 2015).

In the literature, many studies are explaining the relationship between non-destructive testing methods and the properties of concrete (Kolluru et al., 2000). In some of these studies, concrete specimens are prepared with different cementitious materials, and some specimens are stored and cured at different temperatures (Hong et al., 2021). For several studies, even the damage of concrete was individually investigated with various NDT methods (Chun et al., 2020). However, there is no study that seeks to demonstrate the relationship between the damage of the concrete specimens and non-destructive testing methods for concretes with different binders as far as the authors' concern.

In this study, three NDT methods: electrical resistivity, ultrasonic pulse velocity, and resonance frequency were used. Concrete specimens which were prepared with different pozzolans such as fly ash, silica fume, and ground granulated blast furnace slag, were damaged to various levels of their compressive strength value. The extent of the damage was expressed as a percentage of compressive strength of the specimens, ranging from 0% to 100% in increments of 25%. At the end of this study, the relationship between NDT results and damage level of concrete specimens was established.

2. Experimental Program

2.1. Materials and mix design

In this study, the main goal is to find a relation between the degree of damage on a concrete specimen and the results of electrical resistivity, ultrasonic pulse velocity, and resonant frequency tests. For this purpose firstly, the concrete mixtures were designed and specimens were prepared according to ACI 211.1-91 guideline and ASTM C192 standard, respectively (ACI 211.1-91, 2002; ASTM C192 / C192M-14, 2014).

For concrete mix design, a target compressive strength of 25 MPa is specified for the mixture without any cement replacement materials which serves as a control mixture. For the remaining three mixtures some of the Portland cement was replaced with fly ash, silica fume and ground granulated blast furnace slag. The replacement level was based on conventional usage of these binders.

CEM I 42.5 R type ordinary Portland cement (OPC) was a product of Oyak Cement Factory, fly ash (FA) was obtained from Yatağan Thermal Power Plant, silica fume (SF) from Eti Metallurgy Inc. in Antalya, and finally the ground granulated blast furnace slag (GGBFS) from Iskenderun Iron and Steel Plant. The chemical compositions and physical properties of the binding materials are provided in Table 1.

As mentioned previously, 25 MPa compressive strength was targeted in the control mixture. In the mixtures containing FA, SF, and GGBFS produced to investigate the effects of different binder materials, the replacement levels of 20, 5, and 20% were used, respectively. The proportions of the ingredients of produced concretes are presented in Table 2.

2.2. Specimen preparation

For all the compressive strength and NDT tests conducted throughout the experimental research, cylindrical specimens with 10 cm diameter and 20 cm height

were used. During the preparation of the fresh concrete, firstly aggregates and half of the mixing water were introduced to a drum-type concrete mixer. The mixer was operated until the entire surface of the aggregates was wetted. After then, Portland cement, mineral admixtures (if used), and all the remaining mixing water were introduced into the mixer. The mixer was restarted again, and the mixing process was completed when a homogeneous mixture was obtained. Once the fresh concrete was prepared, cylindrical molds with a diameter of 10 cm and a height of 20 cm were filled with fresh concrete in two layers and compacted as seen in Fig. 1.

Table 1. Chemical composition and physical properties of binding materials.

	PC	FA	GGBFS	SF
SiO ₂ (%)	18.69	50.04	38.4	91.96
CaO (%)	61.87	11.21	34.48	0.62
Al ₂ O ₃ (%)	4.74	22.85	10.96	1.20
Fe ₂ O ₃ (%)	3.37	8.02	0.81	0.84
MgO (%)	3.36	2.23	7.14	1.02
SO ₃ (%)	2.93	0.78	1.48	0.12
K ₂ O (%)	0.63	2.50	0.86	1.16
Na ₂ O (%)	0.19	2.27	0.18	0.67
Specific Gravity	3.15	2.28	2.79	2.20
Blaine Fineness (m ² /kg)	342	285	425	-

Table 2. Concrete mix proportions.

	PC (kg/m³)	FA (kg/m³)	SF (kg/m³)	GGBFS (kg/m³)	Coarse aggregate (kg/m³)	Fine aggregate (kg/m³)	Water (kg/m³)
PC-Mix	400	0	0	0	960	714	216
FA-Mix	320	80	0	0	960	619	216
SF-Mix	380	0	20	0	960	621	216
GGBFS-Mix	320	0	0	80	960	636	216



Fig. 1. Cylindrical concrete specimens.

After this process, molds were left for 24 hours under laboratory conditions, then the specimens were removed from the molds and cured under water at 23°C till the age of testing for the development of strength. Afterward, in each mixture, 6 specimens were produced and used for the ages of 7, 28 and 90 days. 3 of the specimens were used as control specimens and the other 3 specimens were used as test specimens. The compressive strength of the specimens in the control group was determined under a constant loading rate of 0.3 MPa/s according to the ASTM C39 as seen in Fig. 2 (ASTM C39, 2021). For the control specimens, NDT measurements were taken from the sound specimens before testing, and also after loading the specimens to failure for each experimental method. For the test group, the specimens were loaded gradually to 0%, 25%, 50%, 75%, and 100% of their compressive strength, and NDT tests were performed prior to loading and also after each level of damage. The damage levels were calculated according to the compressive strength values of control specimens at failure

The electrical resistivity test was carried out at a frequency of 1 kHz of alternating current. To provide the uninterrupted current flow, sponges that were wetted to a constant weight of 21 g were placed between the specimens and the electrode layers. Afterward, as seen in Fig. 3, cylindrical specimens were placed between two electrodes, and the measurements were taken. Then the measured resistance values were used to calculate the electrical resistivity of the specimens.



Fig. 2. Compression test.



Fig. 3. Electrical resistivity test.

The ultrasonic pulse velocity test was carried out at a frequency of 54 kHz. During this test, ultrasound gel was applied as a contact material between transducers and

the specimen. The transmitting and receiving transducers were placed on the parallel surfaces of the concrete specimen and measurements were taken through direct transmission as seen in Fig. 4.





Fig. 4. Ultrasonic pulse velocity test and resonance frequency test.

The resonance frequency test was operated via a resonance frequency meter with maximum sampling frequency of 100 kHz. After the dimensions and mass of specimens are input into the frequency meter, the specimens are struck with a 19 mm diameter-steel ball impactor from one end regarding the longitudinal vibration mode. The specimen vibrations are obtained with the accelerometer from the other end of specimen and the obtained frequency values are measured with frequency meter as seen in Fig. 4.

3. Result and Discussion

3.1. Compressive strength

The compressive strength values in the graph were obtained as a result of compression test applied on control specimens of each mixture till their failure. Depending on the mineral admixtures used in the production of concrete mixtures, as seen in Fig. 5, the development of the compressive strength differs. The compressive strengths of concrete mixtures which were prepared by different mineral admixtures were lower than the control mixture at early ages and similar or higher at later

ages. This situation is expected as they differ in activity and rate of reaction (Shi et al., 2009; Duan et al., 2013; Gonen and Yazicioglu, 2007; Hassan et al., 2000).

The control mixture showed the highest compressive strength only at 7 days due to the rapid hydration of Portland cement compared to other mineral admixtures. Although mixtures apart from the control mixture had similar compressive strengths at early ages, the use of SF resulted in slightly higher strength. This can be attributed to the lower replacement level of SF (5%) compared to FA and GGBFS. However, at the end of the 28th day, the difference became more pronounced in favor of the mixture containing silica fume as it gained a considerably higher strength than the other mixtures. Similar situations were confirmed by several authors in the literature (Ozturk et al., 2020; Gokce et al., 2019; Gupta et al., 2021). Although the compressive strength of concretes containing ground granulated blast furnace slag and fly ash was lower than the control mixtures as of this age, the GGBFS mixture reached a strength close to the control mixture with the effect of high CaO content. At 90 days, SF, and GGBFS mixtures reached higher compressive strength than the control mixture and FA reached a strength close to the control mixture as a result of pozzolanic activity and secondary hydration.

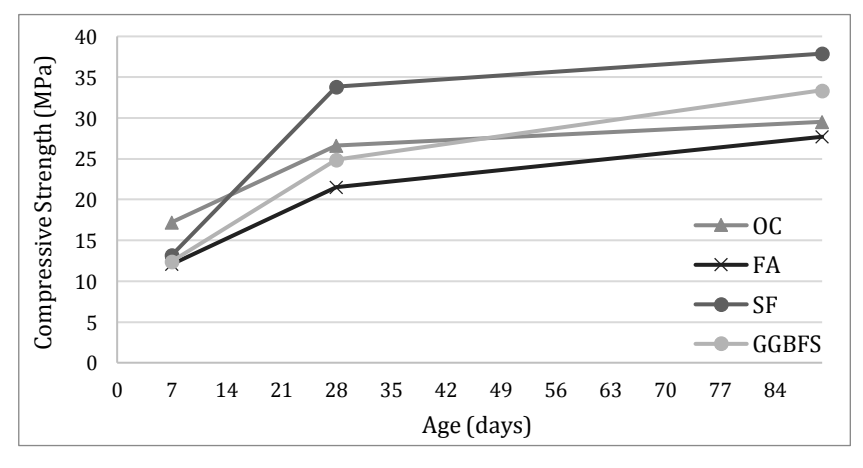


Fig. 5. Compressive strength development.

3.2. Electrical resistivity

For obtaining the electrical resistivity values, the impedance values at the lowermost phase angles were determined. Nevertheless, for the 1 kHz frequency at which the measurements were taken, the phase angles were always 0° hence, impedance values were equal to the resistance. Electrical resistivity could easily be calculated by multiplying the resistance with the cross-sectional area and dividing it by the length of the specimen. When the graph was observed, it should be mentioned that in each mixture, the first, second and third points provide the values for the ages of 7, 28 and 90 days respectively. To distinguish the results, 7 days values were presented with solid filled markers, 28 days values with blank markers and 90 days values with pattern filled markers.

It was understood from the results obtained that the resistivity values increase with age. This situation can be explained by the decrease in the capillary voids as specimen age increases. Similarly, electrical resistivity values also increased in the same manner when the sound specimens were damaged due to the cracks formed as a result of loading. The reason for the increase in resistivity is due to the difficulty of electrical current to pass through the formed cracks and voids when the moisture content is kept constant. Studies showed that electrical resistivity increases with specimen age and compressive strength (Medeiros-Junior et al., 2016; Lübeck et al., 2012; Valcuende et al., 2020; Bem et al., 2018; Ferreira and Jalali, 2010; Duran-Herrera et al., 2019; Ghoddousi and Saabadi, 2017; Tumidajski, 2005; Gastaldini et al., 2009). As seen in Fig. 6, a similar trend is also observed in this study.

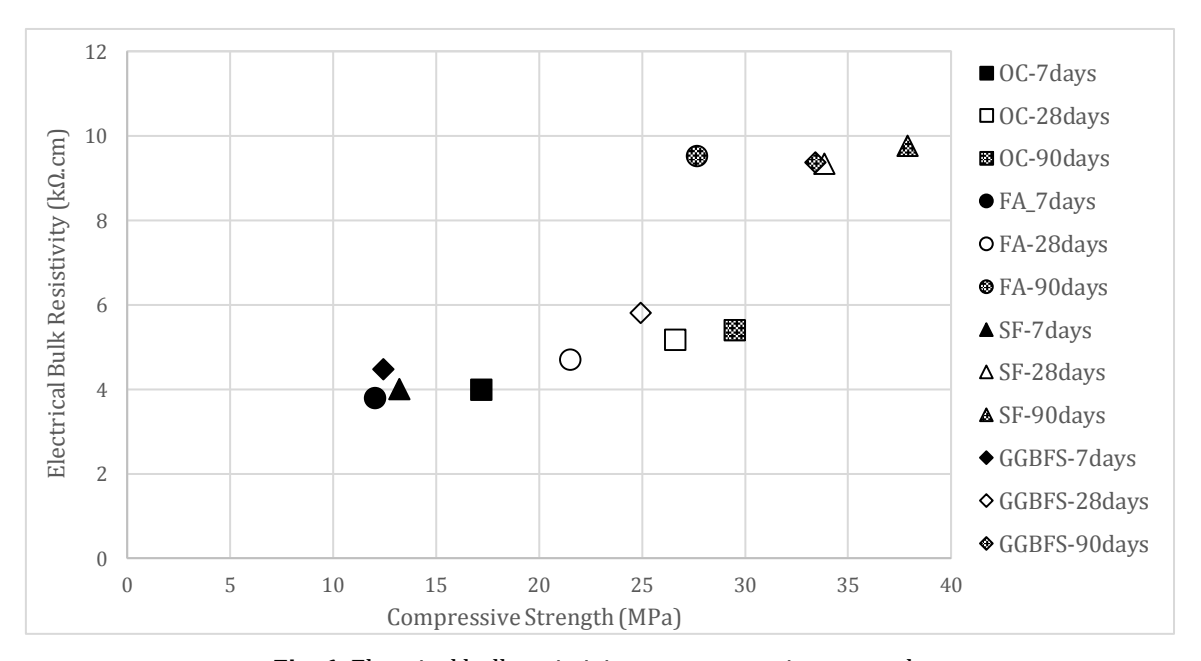


Fig. 6. Electrical bulk resistivity vs. compressive strength.

In addition, the measurement of the electrical resistivity of concrete is realized by the ion transfer through the water-filled pores in the concrete. Since the chemical compositions of the mineral admixtures used in this study are different from ordinary Portland cement as seen in Table 1, the electrical resistivity of the concrete specimens prepared by using them is also different as they alter the chemistry of the pore solution (Duran-Herrera et al., 2019; Gastaldini et al., 2009; Shi, 2004). The electrical resistivities of the control specimens of each mixture for the ages of 7, 28 and 90 days before (undamaged state) and after (failed state) the application of compressive loads up to the failure of the specimens are shown in Fig. 7. Also, the response of electrical resistivity to gradually increased damage levels are shown in Fig. 8.

Electrical bulk resistivity test results revealed that the electrical resistivity values follow the same trend with the compressive strength test results for gradually damaged specimens. For instance, the resistivity values at 7, 28, and 90 days ranged in the same order as the compressive strengths for FA-mix and GGBFS-mix, as seen in Fig. 7. Electrical resistivity tests could not be performed

on some of the specimens as they lost their integrity after being loaded to failure.

However, for OC-mix and especially SF-mix as seen in Fig. 7, the development of electrical resistivity was slow between 28 and 90 days in contrast to the FA-mix and GGBFS-mix. This situation can be explained by the reaction mechanism that causes the early gain of strength in mixtures containing silica fume and Portland cement or Portland cement alone as a binder and the contribution of FA and GGBFS to the strength relatively later.

When the effect of damage condition on resistivity values is examined, it can be said that there was a slight increase in the values for specimens with 25% damage in general. In other words, the electrical resistivity changed for the level of damage where cracks occurred in the interface area between the aggregate and cement mortar. However, this change was not evident in all mixtures and is slight for the mixtures it was observed. Electrical bulk resistivity values generally did not show a significant change at damage levels between 25% and 75%, where matrix cracks begin to form and develop, while it increases in the damage level between 75% and 100%.

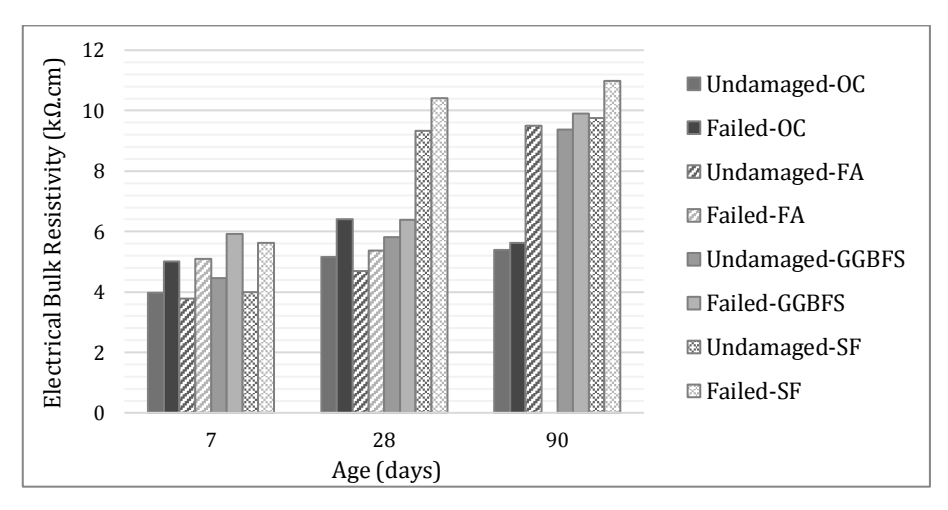


Fig. 7. Electrical bulk resistivity vs. age for each mixture.

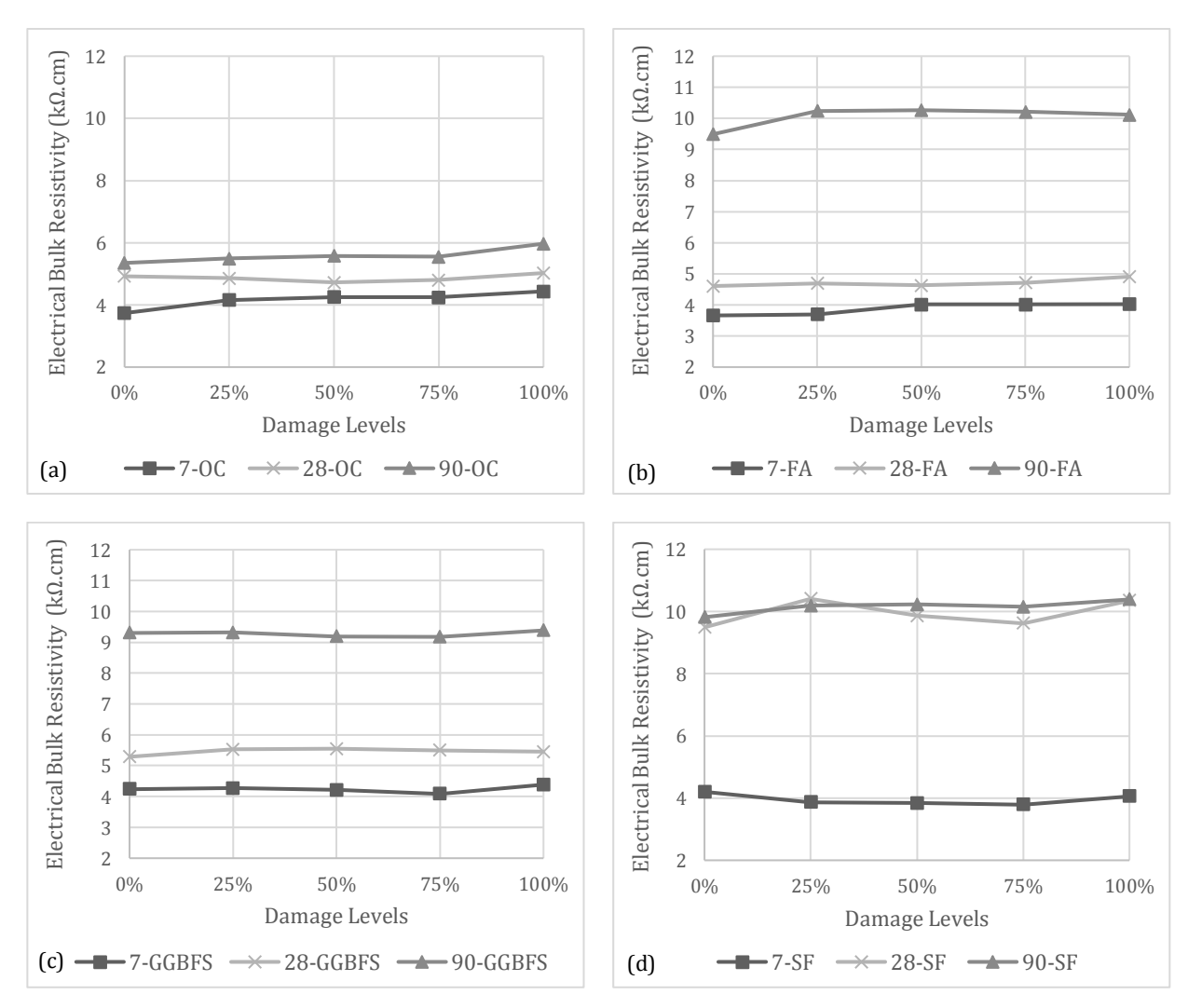


Fig. 8. Electrical bulk resistivity vs. damage levels for each mixture.

3.3. Ultrasonic pulse velocity

In general, ultrasonic pulse velocity values increased with the age of specimens. When observed, the first, second and third points provided the values for the ages of 7, 28 and 90 days respectively in each mixture. To avoid any confusion in the graph, solid filled, blank and pattern

filled markers were used to demonstrate 7, 28 and 90 days values. As seen in Fig. 9, the increase in compressive strength depending on the age of the specimen also resulted in an increase in the ultrasonic pulse velocity. The reason for the increase in ultrasonic pulse velocity as the age increases can be regarded as the continuation of the hydration reactions in the concrete and the filling of the

voids in the concrete with C-S-H gels as a result of the hydration reactions. Various studies (Trtnik et al., 2009; Tanyildizi and Coskun, 2008; Lai et al., 2001; Lee and Lee, 2020; Demirboğa et al., 2004; Godinho et al., 2020) have also concluded that the ultrasonic pulse velocity increases when the concrete gains compressive strength.

The ultrasonic pulse velocity values of the control specimens of each mixture for the ages of 7, 28 and 90 days before (undamaged state) and after (failed state) the application of compressive loads up to the failure of the specimens are shown in Fig. 10. Change in the ultrasonic pulse velocity values depending on damage levels is provided in Fig. 11 for each mixture.

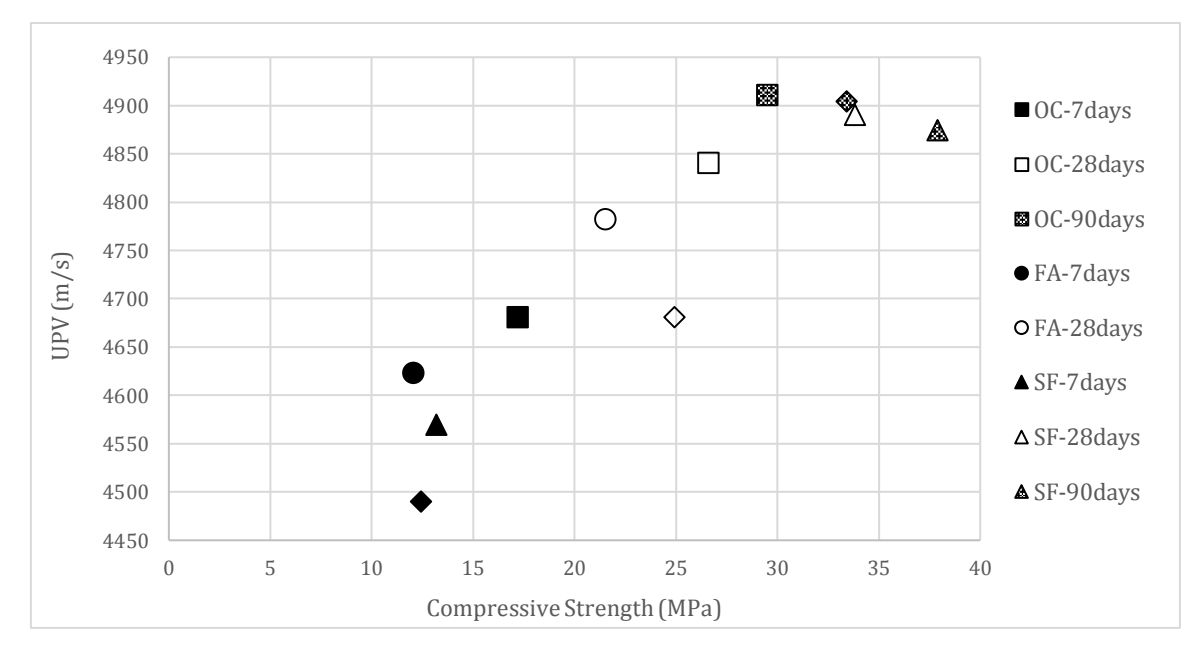


Fig. 9. Ultrasonic pulse velocity vs. compressive strength.

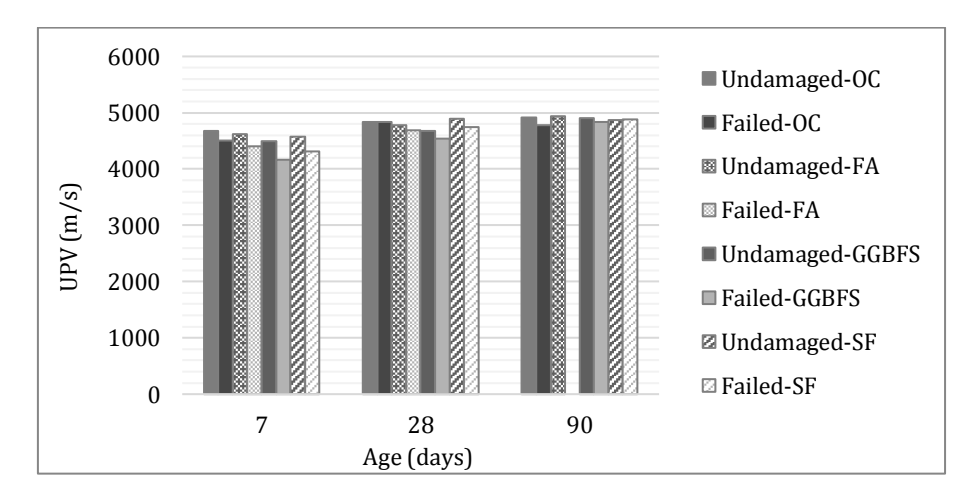


Fig. 10. Ultrasonic pulse velocity vs. age for each mixture.

Ultrasonic pulse velocity results for the OC-mix are given in Fig. 10 and Fig. 11(a). It can be interpreted that the ultrasonic pulse velocity increases as the age of the concrete increases for this mixture. In addition, depending on the extent of concrete damage, decreases in ultrasonic pulse velocity can be mentioned.

In Figs. 10 and 11 ultrasonic pulse velocity developments, depending on age and damage, of FA and SF mixtures can be observed. Since ultrasonic pulse waves cannot pass through the voids inside the concrete, they pass around the voids following a more tortuous path and therefore travel a longer distance. This situation causes a decrease in the ultrasonic pulse velocity of the early

age concrete specimen. When the specimens are loaded, the ultrasonic pulse velocity values also decrease. This is because, due to crack formation in the specimen, ultrasonic waves have to travel a longer distance as they go around the cracks.

Ultrasonic pulse velocity results for the GGBFS-mix are given in Figs. 10 and 11(c). It can be interpreted that the ultrasonic pulse velocity increases as the age of the concrete increases for this mixture just as OC-mix. Additionally, depending on the extent of concrete damage, decreases in ultrasonic pulse velocity can be mentioned as well.

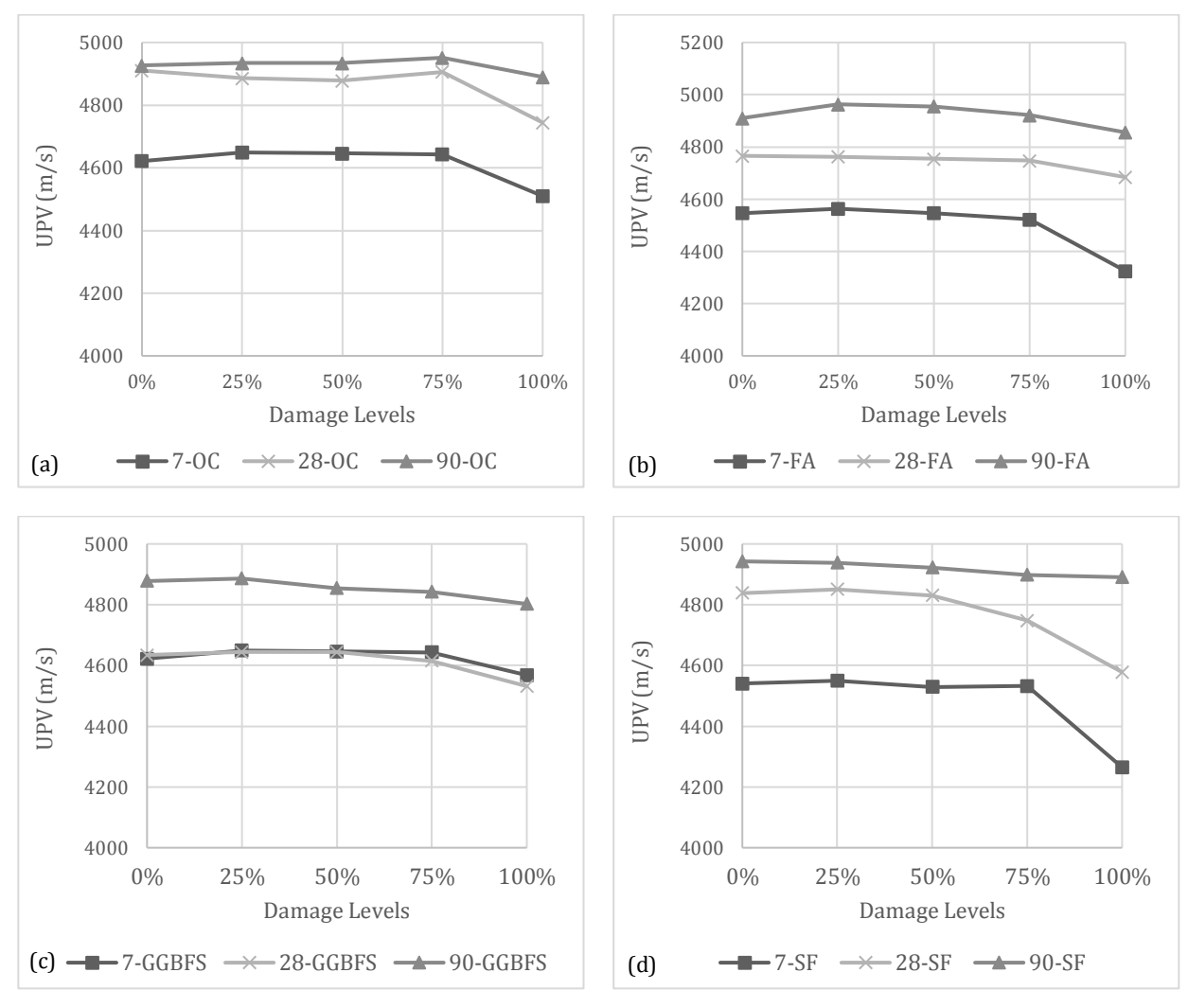


Fig. 11. Ultrasonic pulse velocity vs. damage levels for each mixture.

The ultrasonic pulse velocity showed little variation in gradually damaged concrete specimens regardless of the test age. However, a significant decrease in ultrasonic pulse velocity is observed for all mixtures in the 75%-100% damage level range where matrix cracks develop. From this decrease, it can be concluded that ultrasonic waves pass through the matrix in intact samples and the crack path lengthens only with the increase in the number of cracks in the matrix.

Another inference that can be obtained from the UPV test results is that the velocity decrease for specimens tested at an early age is more significant than in specimens tested at a later age. This may indicate that more matrix cracks occur in low-strength concrete specimens at the same level of damage than high-strength specimens.

3.4. Resonance frequency

Aside from the other NDT tests conducted in this study, resonant frequency measurements could not be conducted at 7 days. For this reason, results were evaluated based on the measurements taken at 28 and 90 days. Dynamic modulus of elasticity values were calculated by using longitudinal resonance frequencies in accordance with ASTM C215 standard. Since the specimen

properties are similar, longitudinal resonance frequencies and dynamic modulus of elasticity values can be evaluated in the same way. Dynamic modulus of elasticity was calculated by using Eq. (1).

$$Dynamic E = DM(n')^2 \tag{1}$$

where M is the mass of specimen; n' is the fundamental longitudinal frequency (Hz); and D is $5.093 \cdot (L/d^2)$ (m⁻¹) for a cylinder, or $4 \cdot (L/bt)$ (m⁻¹) for a prism.

In the graph below, it should be mentioned that in each mixture, the first and second points provide the values for the ages of 28 and 90 days respectively. To separate the ages, 28 days and 90 days values were shown with blank and pattern filled markers individually. As seen in Fig. 12, the dynamic elasticity modulus that was obtained from the resonance frequency test, as in the ultrasonic pulse velocity test, increased proportionally with the compressive strength of the concrete.

The aged concrete specimens showed a higher dynamic modulus of elasticity as a result of continuous hydration reactions in the concrete and as the existing pores in the concrete are filled with C-S-H gels. Researchers (Lee et al., 1997; Giner et al., 2011) also observed in their study that as the compressive strength of concrete increases, the dynamic modulus of elasticity increases.

The dynamic elastic modulus values of the control specimens of each mixture for the ages of 28 and 90 days before (undamaged state) and after (failed state) the application of compressive loads up to the failure of the

specimens are shown in Fig. 13. Variations in the dynamic modulus of elasticity velocity values depending on damage levels are provided in Fig. 14.

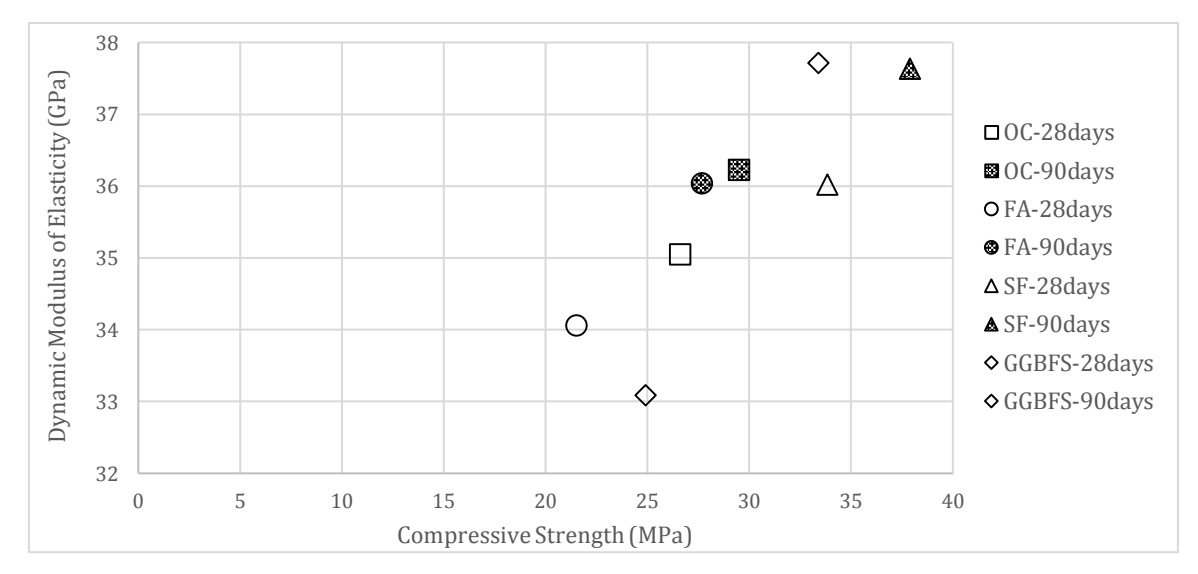


Fig. 12. Dynamic modulus of elasticity vs. compressive strength.

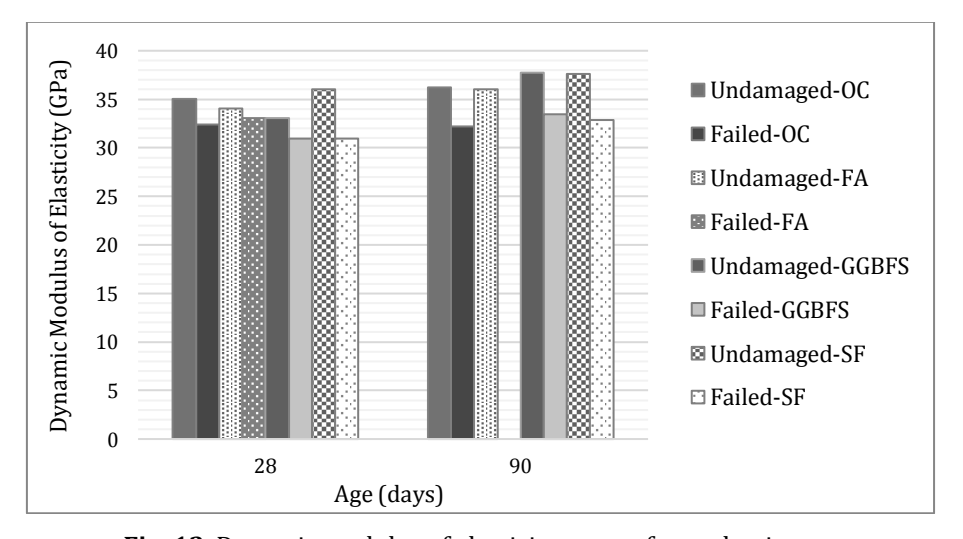


Fig. 13. Dynamic modulus of elasticity vs. age for each mixture.

Considering all the results, the dynamic elasticity modules were obtained from the resonance frequency test results showed a decrease even at the lowest damage level for all concrete mixtures, unlike the electrical resistivity and ultrasonic pulse velocity test results. This decrease is sustained proportional to the damage level, up to the 75% damage level, where interface cracks form and develop and matrix cracks begin to form. This situation is observed regardless of the concrete strength and the binder materials used. In this respect, the resonance frequency test stands out compared to other methods for determining low damage levels. On the other hand, for damage levels between 75% and 100%, the amount of decrease in the dynamic elastic modulus becomes more prominent and observable in all mixtures regardless of concrete strength and binding material type.

When all the results are evaluated together, the most accurate method of measuring concrete damage emerges as the resonance frequency test. For this reason, the diagram given in Fig. 15 was created in order to evaluate the extent of damage depending on the change in the dynamic modulus of elasticity independent of the dynamic elasticity modulus at the undamaged state and therefore the type of binder. As can be seen from the Fig. 15, the dynamic modulus of elasticity obtained from the resonance frequency test immediately decreases even after low damage. With the help of the data presented in the diagram, a third-degree polynomial was drawn to the data in order to obtain the damage amount by using the dynamic elastic modulus values.

When Fig. 15 is inspected it is seen that the vertical axis is between 86 to 100%. This type of presentation is pre-

ferred to make it easier for the reader to understand how the polynomial fits the data. If the vertical axis is chosen between a wider range, it will not be possible to see how the polynomial fits the data. In addition, it is obvious that as the extent of loading increases the data becomes scattered as up to 50% loading a stable system of microcracks form, only after 50-60% cracks start to form in the matrix and after 75% of interfacial zone becomes unstable and propagation of cracks increase in the matrix and finally spontane-

ous cracks grow (Mehta and Monteiro, 2006). This is the reason for obtaining a wider data at higher load levels.

Considering the results of all the tests conducted within the scope of this study, electrical resistance and ultrasonic pulse velocity can be used to evaluate the damage of concrete, but the most accurate results can be obtained with the resonance frequency test. The use of resonance frequency test will give more precise results for low damage amount due to higher sensitivity.

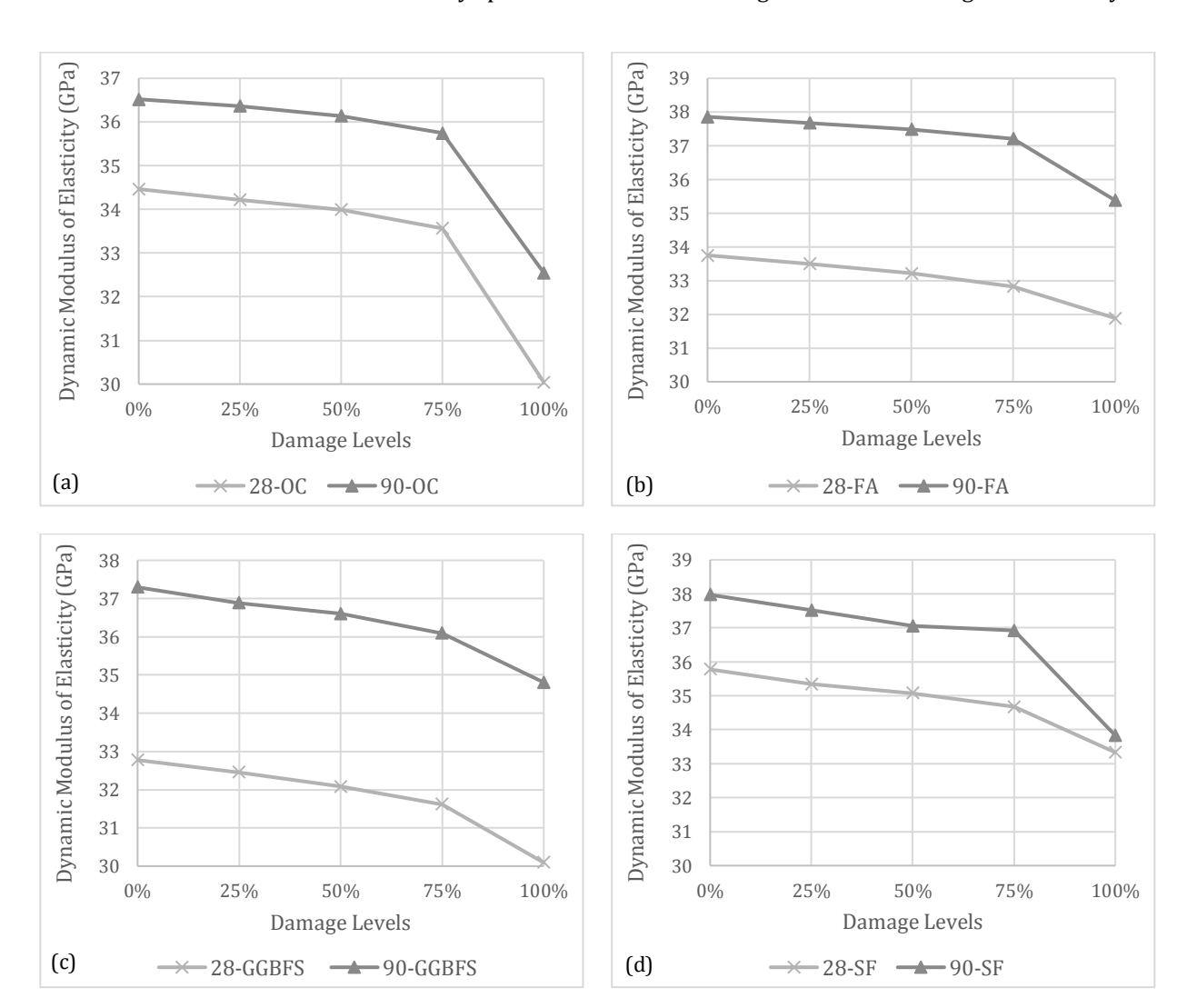


Fig. 14. Dynamic modulus of elasticity vs. damage levels for each mixture.

4. Conclusions

The following conclusions were drawn from the results of the tests conducted throughout the study:

- At the end of the 7th day, the mixture that only contained ordinary Portland cement as a binder showed
 the highest compressive strength as a result of rapid
 hydration of cement compared to the other mineral
 admixtures. However, the gap decreased after 28
 days.
- Similar to compressive strength, bulk electrical resistivity results also increased with specimen age as concrete pores are filled with hydration products. Failed specimens had higher bulk electrical resistivities than undamaged specimens as void volume in-

- creased, and water saturation of the voids decreased
- Bulk electrical resistivity results were also changed when specimens were gradually damaged. Between 75% and 100% damage levels, a significant increase was observed in the bulk electrical resistivity.
- Similar to the bulk electrical resistivity, ultrasonic pulse velocity increased with the age of the specimen. As cracks increased in number and volume in damaged concrete, a decrease was observed in the pulse velocity. Similarly, ultrasonic pulse velocity significantly decreased between 75% and 100% damage levels. The extent of this decrease was higher at early ages probably as matrix cracks occur at lower levels of damage in lower strength concrete.

 Contrary to electrical bulk resistivity and ultrasonic pulse velocity, dynamic modulus of elasticity values continually declined up to 75% damage level. This decrease can be explained as cement matrix cracks started to occur and develop. This indicates that resonant frequency potentially predicts the damage level better compared to the other methods. The decrease became more prominent between 75% and 100% damage levels regardless of binding materials and compressive strength of the concrete specimens which makes the resonance frequency test a useful tool to predict the extent of concrete damage.

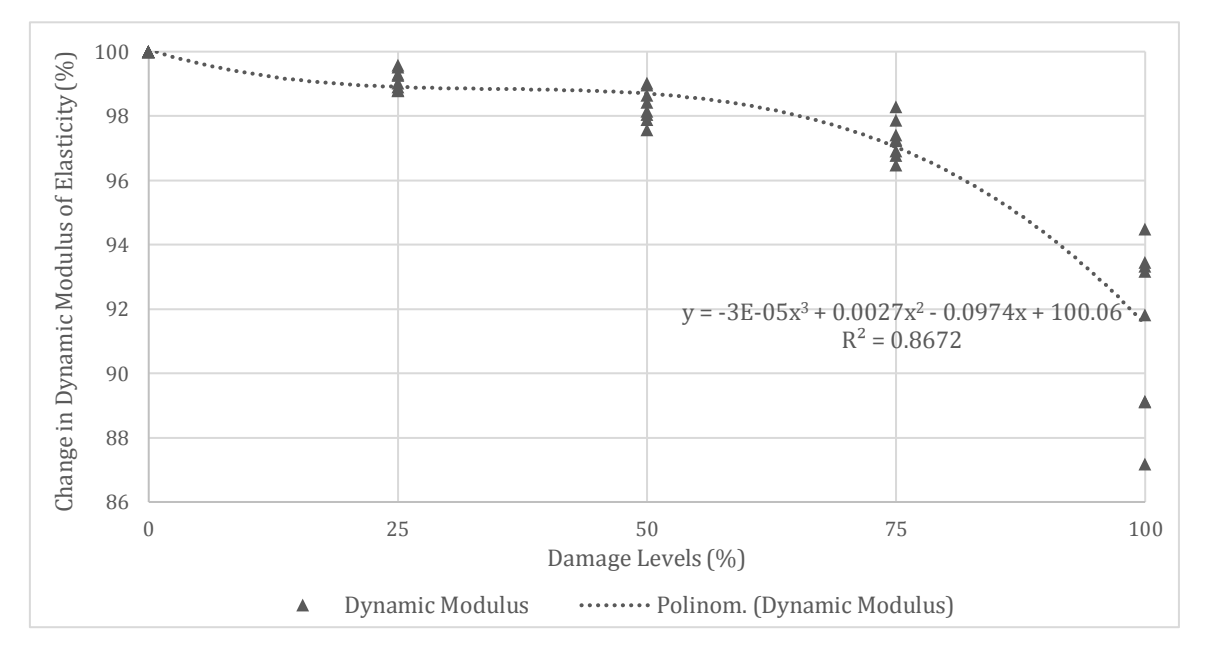


Fig. 15. Change in dynamic modulus vs. damage levels.

Acknowledgements

This study was funded and supported by the Scientific and Technological Research Council of Turkey (TÜ-BİTAK) under "2020/1 2209-A - Research Project Support Programme for Undergraduate Students" (Application number: 1919B012001306).

REFERENCES

ACI 211.1-91 (2002). Standard Practice for Selecting Proportions for Normal Heavyweight, and Mass Concrete. American Concrete Institute, Farmington Hills, Michigan, USA.

ACI 228.2R-98 (1998). Nondestructive Test Methods for Evaluation of Concrete in Structures. American Concrete Institute, Farmington Hills, Michigan, USA.

ASTM C39 / C39M-21 (2021). Standard Test Method for Compressive Strength of Cylindrical Concrete Specimens. ASTM International, West Conshohocken, PA, USA.

ASTM C192 / C192M-14 (2014). Standard Practice for Making and Curing Concrete Test Specimens in the Laboratory. ASTM International, West Conshohocken, PA, USA.

ASTM C215-08 (2008). Standard Test Method for Fundamental Transverse, Longitudinal, and Torsional Frequencies of Concrete Specimens. ASTM International, West Conshohocken, PA, USA.

ASTM C597-97 (1997). Standard Test Method for Pulse Velocity through Concrete. ASTM International, West Conshohocken, PA, USA.

Bem DH, Lima DPB, Mederios-Junior RA (2018). Effect of chemical admixtures on concrete's electrical resistivity. *International Journal of Building Pathology and Adaptation*, 36 (1), 174-187.

Breysse D (2012). Non-Destructive Assessment of Concrete Structures: Reliability and Limits of Single and Combined Techniques. *Springer*, Dordrecht, Netherland.

Chun P, Ujike I, Mishima K, Kusumoto M, Okazaki S (2020). Random Forest-based evaluation technique for internal damage in reinforced concrete featuring multiple nondestructive testing results. *Construction and Building Materials*, 253, 119238.

Demirboğa R, Türkmen İ, Karakoç MB (2004). Relationship between ultrasonic velocity and compressive strength for high-volume mineral-admixtured concrete. *Cement and Concrete Research*, 34, 2329-2336.

Duan P, Shui Z, Chen W, Shen C (2013). Efficiency of mineral admixtures in concrete: Microstructure, compressive strength and stability of hydrate phases. *Applied Clay Science*, 83-84, 115-121.

Duran-Herrera A, De-León-Esquivel J, Bentz DP, Valdez-Tamez P (2019). Self-compacting concretes using fly ash and fine limestone powder: Shrinkage and surface electrical resistivity of equivalent mortars. Construction and Building Materials, 199, 50-62.

Ferreira RM, Jalali S (2010). NDT measurements for the prediction of 28-day compressive strength. *NDT&E International*, 43, 55-61.

Gastaldini ALG, Isaia GC, Hoppe TF, Missau F, Saciloto AP (2009). Influence of the use of rice husk ash on the electrical resistivity of concrete: A technical and economic feasibility study. *Construction and Building Materials*. 23, 3411-3419.

Ghoddousi P, Saabadi LA (2017). Study on hydration products by electrical resistivity for self-compacting concrete with silica fume and metakaolin. Construction and Building Materials, 154, 219-228.

Giner VT, Ivorra S, Baeza FJ, Zornoza E, Ferrer B (2011). Silica fume admixture effect on the dynamic properties of concrete. *Construction and Building Materials*, 25, 3272-3277.

Godinho JP, De Souza TF, Medeiros MHF, Silva MA (2020). Factors influencing ultrasonic pulse velocity in concrete. *IBRACON Structures and Materials Journal*, 13, 222-247.

Gokce HS, Hatungimana D, Ramyar K (2019). Effect of fly ash and silica fume on hardened properties of foam concrete. *Construction and Building Materials*, 194, 1-11.

- Gonen T, Yazicioglu S (2007). The influence of mineral admixtures on the short and long-term performance of concrete. *Building and Environment*. 42, 3080-3085.
- Gupta M, Raj R, Sahu AK (2021). Effect of Rice Husk Ash, silica fume & GGBFS on compressive strength of performance based concrete. *Materials Today: Proceedings*.
- Hassan KE, Cabrera JG, Maliehe RS (2000). The effect of mineral admixtures on the properties of high-performance concrete. *Cement and Concrete Composites*, 4, 267-271.
- Helal J, Sofi M, Mendis P (2015). Non-destructive testing of concrete: A review of methods. *Electronic Journal of Structural Engineering*, 14(1), 97-105.
- Hong G, Oh S, Choi S, Chin WJ, Kim YJ, Song C (2021). Correlation between the Compressive Strength and Ultrasonic Pulse Velocity of Cement Mortars Blended with Silica Fume: An Analysis of Microstructure and Hydration Kinetics. *Materials*, 14, 2476.
- Kolluru SV, Popovics JS, Shah SP (2000). Determining Elastic Properties of Concrete Using Vibrational Resonance Frequencies of Standard Test Cylinders. *Cement, Concrete, and Aggregates,* CCAGDP, 22 (2), 81-89.
- Lai C, Lin Y, Yen T (2001). Behavior and Estimation of Ultrasonic Pulse Velocity in Concrete. Structural Engineering, Mechanics and Computation, 2, 1365-1372.
- Layssi, G, Ghods, P, Alizadeh, AR, Salehi, M (2015). Electrical Resistivity of Concrete, Concrete International, 37, 5.
- Lee KM, Kim DS, Kim JS (1997). Determination of dynamic Young's modulus of concrete at early ages by impact resonance test. KSCE Journal of Civil Engineering, 1, 11-18.
- Lee T, Lee J (2020). Setting time and compressive strength prediction model of concrete by nondestructive ultrasonic pulse velocity testing at early age. *Construction and Building Materials*, 252.
- Lübeck A, Gastaldini ALG, Barin DS, Siqueira HC (2012). Compressive strength and electrical properties of concrete with white Portland cement and blast-furnace slag. Cement and Concrete Composites, 34, 392-399.
- Medeiros-Junior RA, Lima MG (2016). Electrical resistivity of unsaturated concrete using different types of cement. *Construction and Building Materials*, 107, 11-16.
- Mehta PK and Monteiro PJM (2006). Concrete: Microstructure, Properties, and Materials. 3rd Edition. McGraw-Hill, New York.

- Mohammed TU, Mahmood AH (2016). Effects of maximum aggregate size on UPV of brick aggregate concrete. *Ultrasonics*, 69, 129-136.
- Ozturk M, Karaaslan M, Akgol O, Sevim UK (2020). Mechanical and electromagnetic performance of cement based composites containing different replacement levels of ground granulated blast furnace slag, fly ash, silica fume and rice husk ash. *Cement and Concrete Research*, 136.
- Qasrawi HY (2000). Concrete strength by combined nondestructive methods simply and reliably predicted. Cement and Concrete Research. 30, 739-746.
- Shane JD, Aldea CM, Bouxsein NF, Mason TO, Jenning HM, Shaw SP (1999). Microstructural and pore solution changes induced by rapid chloride permeability test measured by impedance spectroscopy. Concrete Science and Engineering, 1, 110-119.
- Shi C (2004). Effect of mixing proportions of concrete on its electrical conductivity and the rapid chloride permeability test (ASTM C1202 or ASSHTO T277) results. *Cement and Concrete Research*, 34, 537-545.
- Shi H, Xu B, Zhou X (2009). Influence of mineral admixtures on compressive strength, gas permeability and carbonation of high performance concrete. *Construction and Building Materials*, 23, 1980-1985.
- Tanyildizi H, Coskun A (2008). Determination of the principal parameter of ultrasonic pulse velocity and compressive strength of lightweight concrete by using variance method. *Russian Journal of Non-destructive Testing*, 44, 639-646.
- Trtnik G, Kavčič F, Turk G (2009). Prediction of concrete strength using ultrasonic pulse velocity and artificial neural networks. *Ultrasonics*, 49, 53-60
- Tumidajski PJ (2005). Relationship between resistivity, diffusivity and microstructural descriptors for mortars with silica fume. *Cement and Concrete Research*, 35, 1262-1268.
- Valcuende M, Calabuig R, Martínez Ibernó A, Soto J (2020). Influence of Hydrated Lime on the Chloride-Induced Reinforcement Corrosion in Eco-Efficient Concretes Made with High-Volume Fly Ash. *Materials*, 13 (22), 5135.
- Yildirim G, Aras GH, Banyhussan QS, Şahmaran M, Lachemi M (2015). Estimating the self-healing capability of cementitious composites through non-destructive electrical-based monitoring. NDT&E International, 76, 26-37.